

Conception of myeloperoxidase inhibitors derived from flufenamic acid by computational docking and structure modification

Pierre Van Antwerpen,^a Martine Prévost,^b Karim Zouaoui-Boudjeltia,^c Sajida Babar,^c I. Legssyer,^c Patrick Moreau,^a Nicole Moguilevsky,^d Michel Vanhaeverbeek,^c Jean Ducobu,^e Jean Nève^a and François Dufrasne^{a,*}

^aLaboratory of Pharmaceutical Organic Chemistry, Institut de Pharmacie, Université Libre de Bruxelles, 1050 Brussels, Belgium

^bLaboratory of Structure and Function of Biological Membranes, Université Libre de Bruxelles, 1050 Brussels, Belgium

^cLaboratory of Experimental Medicine, CHU Charleroi Hospital A. Vésale, Université Libre de Bruxelles, 6110 Montigny-le-Tilleul, Belgium

^dTechnology Transfer Office, FUNDP, 5000 Namur, Belgium

^eDepartment of Internal Medicine, CHU Tivoli, Université Libre de Bruxelles, 7100 La Louvière, Belgium

Received 5 September 2007; revised 30 October 2007; accepted 7 November 2007

Available online 13 November 2007

Abstract—The development of myeloperoxidase (MPO) inhibitors has been conducted using flufenamic acid as a lead compound. Computational docking of the drug and its analogs in the MPO active site was first attempted. Several molecules were then synthesized and assessed using three procedures for the measurement of their inhibiting activity: (i) the taurine assay, (ii) the accumulation of compound II, and (iii) the LDL oxidation by ELISA. Most of the synthesized molecules had an activity in the same range as flufenamic acid but none of them were able to inhibit the MPO-dependent LDL oxidation. The experiments however gave some useful indications for a rational conception of MPO inhibitors.

© 2007 Elsevier Ltd. All rights reserved.

1. Introduction

Myeloperoxidase (MPO) is a key enzyme belonging to the complex defense system against exogenous aggressions. It is mostly localized in the azurophil (primary) granules of neutrophils and, in minor proportions, in monocytes. Its role is to ensure the production of hypochlorous acid (HOCl) in presence of hydrogen peroxide (H₂O₂) and chlorine anions (Cl⁻). During phagocytosis, the MPO/H₂O₂/Cl⁻ system promotes the elimination of microorganisms by HOCl-mediated oxidations.¹ However, MPO is liable to be released in extracellular fluids during an oxidative stress and this so-called ‘circulating’ MPO has been suggested to be involved in different pathogenic conditions such as those of chronic inflam-

matory syndromes, atherosclerosis, end-stage renal disease or neurodegenerative diseases.^{2–4}

In this context, several authors have pointed out that the development of efficient MPO inhibitors could be a valuable way to block the potentially harmful enzymatic activity. Some members of our research group already devoted attention to the involvement of MPO in atherosclerosis. Indeed, the enzyme is able to bind to LDL and specifically oxidize apolipoprotein B-100 (ApoB-100), a mechanism generally admitted as a pro-atherogenic factor.^{5,6} For example, the oxidized LDL (Mox-LDL) induces pro-inflammatory responses in endothelial cells and monocytes.⁷ Furthermore, MPO can oxidize the apolipoprotein AI of HDL, leading to a decrease in the cholesterol efflux.⁸ However, the development of MPO inhibitors has so far been undertaken by a few groups with only a limited success.^{9,10}

In the present paper, flufenamic acid (**1**, (2-[(3-trifluoromethylphenyl)amino]benzoic acid, Fig. 1)) was selected

Keywords: Myeloperoxidase; Flufenamic acid; Molecular docking; LDL; Chronic inflammatory diseases.

* Corresponding author. Tel.: +32 26505235; fax: +32 26505249; e-mail: dufrasne@ulb.ac.be

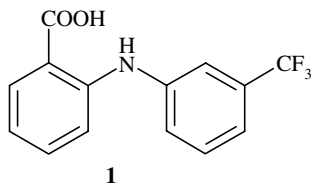


Figure 1. Flufenamic acid structure.

as a lead compound in a process aiming to design MPO inhibitors. This drug that has anti-inflammatory properties linked to cyclooxygenase (COX) inhibition has indeed been reported as an efficient inhibitor of the chlorinating activity of MPO at a micromolar range during the screening of compounds belonging to the same therapeutic class.¹¹ Van Antwerpen et al. confirmed this observation and established that the molecule was directly oxidized by the enzyme in its 5-hydroxy- and 5-chloro-derivatives.¹² As several X-ray crystallographic structures for MPO with various ligands are now available in the scientific literature, it becomes possible to investigate the way flufenamic acid inhibits MPO activity and prevents the interaction of H₂O₂ and/or Cl⁻ with the heme moiety.^{13,14}

A rational drug design process based on the three-dimensional (3D) structure of the target gives the possibility to design and evaluate large series of ligands in terms of affinity. X-ray crystal structures of ligand–protein complexes along with computational analysis tools have been successful in the discovery and optimization of drug candidates¹⁵ and a large number of structure-based drug design programs have been developed in the last 20 years based on a variety of search algorithms according to two main approaches: the fragment-based design and the full-molecule docking. The latest often resorts to compound libraries which are screened for ligands in agreement with the binding site requirements, while the first one uses small molecules with few chemical functionalities positioned in the receptor binding site, which are subsequently grown or assembled into an entire molecule. As the structure of human MPO complexed with cyanide and thiocyanate has already been resolved to 1.9 Å by X-ray crystallography,¹³ computational docking of flufenamic acid and analogs was performed in the MPO active site after validation of the docking procedure. Several molecules were then synthesized and assessed, using three procedures able to measure the potential activity of the inhibitors: (i) the taurine assay,^{11,12} (ii) the accumulation of compound II,^{11,12} and (iii) the LDL oxidation by ELISA.¹⁶

2. Results and discussion

2.1. Docking

2.1.1. Validation. The software Glide[®] is widely used to dock complete molecules into a protein binding site. It has been shown to reproduce experimentally binding poses for a large number of protein targets.¹⁷ However, the most successful docking programs generally produce

a success rate of about 80%. To assess the reliability of the selected procedure, salicylhydroxamic acid (SHA), cyanide (CN⁻), and thiocyanate (SCN⁻) ligands were docked in the binding site of MPO after removal of all water molecules and ligands. The docked poses were compared with the positions of the crystal ligands by computing the root-mean-square deviation (rmsd) which measures the distance between them. A crystal structure of SHA bound to MPO was published in 1996.¹⁴ The structure was not deposited in the PDB but was made available to us by one of the authors (Davey C., private communication). By comparing the predicted poses with the crystal structure and its description in the publication (Fig. 2), a rmsd of the atomic positions of the low-energy pose and the experimental structure of 0.49 Å was obtained, and indicated a high similarity. In accordance with the experimental structure, the hydrophobic moiety of SHA binds in a pocket lined by the pyrrole ring D, Arg239 and the Phe99, 366 and 407. The plane of the aromatic ring is almost parallel to the heme pyrrole ring. This aromatic moiety also interacts with the neighboring Phe99, 366, 407 whose distances vary between 3.9 and 4.8 Å. The hydroxamic acid group lies at the center of the distal cavity between the distal His95 and the heme iron. The carbonyl and hydroxyl oxygens form hydrogen bonds with the protein. The carbonyl oxygen hydrogen bonds to Gln91 side chain and the hydroxyl oxygen of the hydroxamic function forms a hydrogen bond with His95. The salicylic ring hydroxyl group hydrogen bonds to Arg239 side chain. All these interactions are in agreement with the experimental description of the crystal structure. Interestingly, the oxygens of the two hydroxyl and of the carbonyl groups occupy the same positions as the water molecules in the native structure (PDB code:

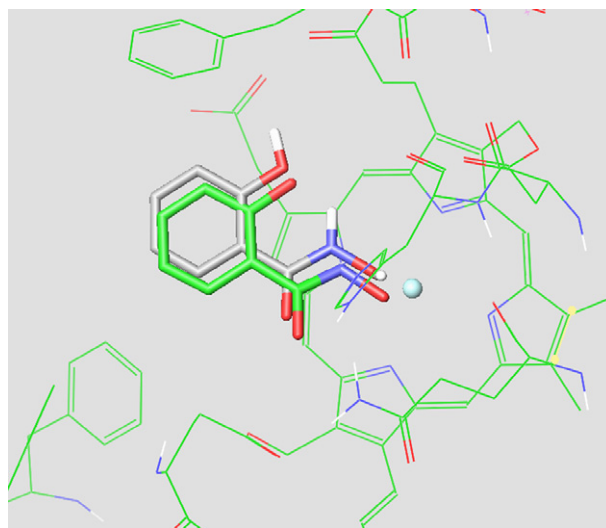


Figure 2. Best pose of the SHA molecule generated by the Glide[®] docking program. For sake of comparison the experimental structure of SHA (Davey CA, private communication and Ref. 26) is also shown. The ligands are depicted as sticks (the experimental structure with gray carbons and the docked structure with green carbons); neighboring residues and the heme are represented as thinner lines. The small blue sphere indicates the location of the Fe ion at the center of the heme.

1CXP). Only one docking pose for CN^- is predicted by Glide. This position reproduces well the crystal position of CN^- with a rmsd of 0.37 Å. In contrast, Glide was not able to reproduce the crystal position of SCN^- . The docked poses are located at the crystal positions of CN^- instead of that of SCN^- . To more accurately reproduce the crystal position of SCN^- (rmsd = 0.77 Å), the ligand had to be docked in the presence of two crystal water molecules present in the crystal structure of protein– SCN^- complex (water molecules numbered 209 and 210 in the crystal structure; PDB code: 1DNU). Thus, the binding mode of SHA and CN^- was identified by docking as well as that of SCN^- providing the presence of two crystal water molecules. The docking procedure could therefore be applied to flufenamic acid and analogs.

2.1.2. Docking of flufenamic acid and analogs. Eight out of 10 poses of flufenamic acid in the MPO binding site correspond to a configuration in which one of the oxygens of the carboxyl group of flufenamic acid matches the crystal position of the sulfur atom in SCN^- , featuring the coincidence of the negative charge of the two ligands (Fig. 3A). The aromatic moiety of the flufenamic acid, bearing the carboxylic group, features an offset stacked geometry with the pyrrole D cycle of the heme and one edge-to-face geometry with Phe99. In these poses, the oxygen of the carboxyl group occupies the position of one crystal water molecule in the native structure. One slightly less energetically favorable pose, due to a few unfavorable van der Waals contacts, corresponds to a location of the carboxyl group shifted more toward the CN^- in which the oxygens of the carboxylate group occupy the crystal positions of the nitrogens of CN^- and SCN^- , respectively (Fig. 3B). Interestingly in that pose, both oxygens reside close to the positions of

two crystal water molecules in the native structure. In the latter pose, the stacking with the pyrrole D ring is more pronounced with an almost face-to-face stacked interaction.

In an attempt to generate a flufenamic acid derivative featuring a better affinity, an *ortho*-diacid compound (compound **2**) was designed. The rationale behind this compound arises from the poses obtained for flufenamic acid and from the observation that MPO binding site can accommodate two negatively charged small ligands, namely CN^- and SCN^- . Another reason for proposing compound **2** comes from the fact that SHA, which binds to the MPO active site, contains two adjacent hydrogen bond acceptors. The diacid compound was thus docked as three forms which differ by the protonation state of one of the two acidic functions. The first two forms bear a single negative charge. But one adopts several geometries in which the carboxylate group matches the position of the crystal SCN^- and the carboxylic acid that of the CN^- . In these poses, three oxygens of the carboxylic functions occupy the positions of three crystal water molecules. The other strikingly differs with the carboxylate located between SCN^- and CN^- crystal positions and the carboxylic acid group hydrogen bonded to one of the propionate functions of the heme. The poses of the third form, which comprises two negative charges, fit very well the charges of SCN^- and CN^- and exhibits a better affinity than the other two forms (Table 1).

Flufenamic acid derivatives, featuring a halogen atom (Cl, F, Br) or a hydroxyl group at the position 5 (compounds **3a–d**), have also been docked in the binding site. This series was designed from the observation that a molecular surface calculated on the crystal structure reveals a small pocket occupied by a crystal water mole-

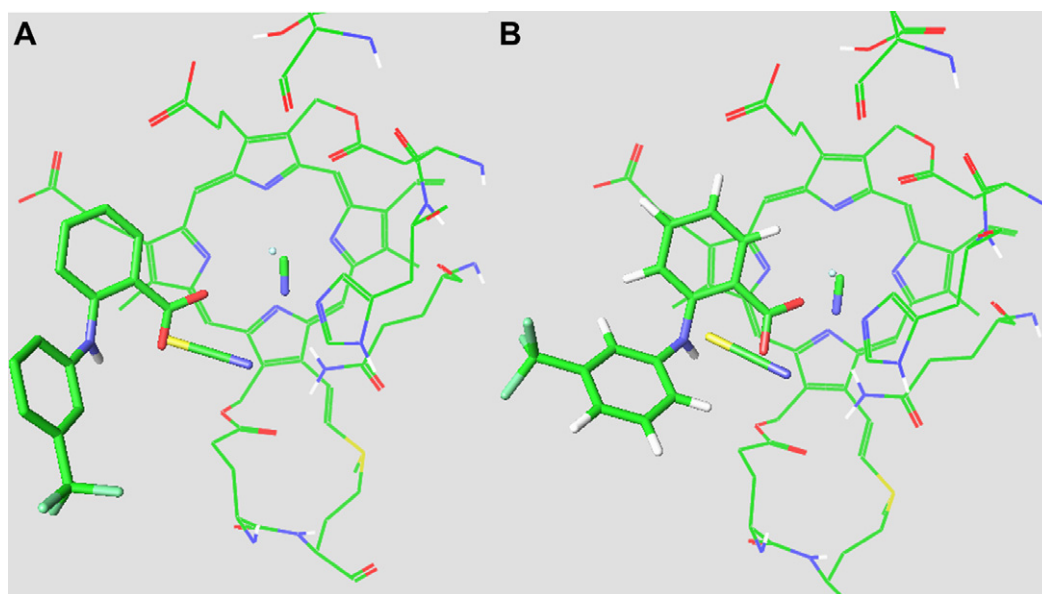


Figure 3. Two best poses of the flufenamic acid molecule. In the first pose (A) the negative charge of the carboxylic acid moiety matches that of the SCN^- in the complexed structure (PDB code: 1DNW). In the second pose (B) the negative charge is located between the positions of SCN^- and CN^- and the two oxygens of the carboxylic function match the locations of two crystal water molecules. The ligand is depicted as sticks; neighboring residues and the heme are represented as thinner lines. The small blue sphere indicates the location of the Fe ion at the center of the heme.

Table 1. ΔG is the predicted free energy of binding from docking experiments; m/z is the ratio of the mass (m) and charge (z); Acc II is the relative value of compound II lifetime in the presence and the absence of chloride, compared to flufenamic acid and the last column lists the experimental IC_{50} for the inhibition of the MPO/H₂O₂/Cl⁻ system

Compound	ΔG (kcal/mol)	m/z	Acc II		IC_{50} (μM)
			Cl ⁻	Without Cl ⁻	
Flufenamic acid (1)	-4.9	281	1	1	1.8 \pm 0.1
Diacid (2)	-6.8 to -4	184 or 369	—	—	>100
Compound 3a (5OH ⁻)	-5.7	297	0	0	n.d.
Compound 3b (5F ⁻)	-4.4	298	2.21	0.91	1.8 \pm 0.5
Compound 3c (5Cl ⁻)	-5.0	315.5	2.42	0.92	1.6 \pm 0.6
Compound 3d (5Br ⁻)	-5.0	360	1.01	0.97	1.8 \pm 0.8
Compound 4a	-4.2	326	7.05	8.26	5 \pm 1
Compound 4b	-5.9	296	0	0	n.d.
Compound 5a	-5.0	338	0.42	1.00	14 \pm 2
Compound 5b	-4.6	304	0.2	0.79	58 \pm 15*
Compound 5c	-7.7	197	0.36	2.53	>100
Compound 5d	-5.9	382	0.10	0.35	>100
Compound 5e	-5.7	381	0.72	0.63	5.5 \pm 0.8

n.d. means that the value could not be calculated as a prooxidant effect was observed. *Significantly different from flufenamic acid ($P < 0.001$, Bonferroni t -test). The range in ΔG given for the diacid compound corresponds to the affinity values obtained for the three forms (see text).

cule and shaped by one of the propionate group of the heme, Arg333, and Arg424. The geometry of interaction of those four compounds is close to that of the flufenamic acid molecule with a coincidence of one of the carboxyl oxygens onto the location of the negative charge of SCN⁻ (Fig. 4). The halogen atom or the hydroxyl group fits well into the pocket previously described (Fig. 4). Only one pose obtained for the fluoro compound is similar to the CN⁻-shifted pose obtained with

flufenamic acid. This might be due to the size of F compared to Cl, Br, and OH.

The compound **4** and **5** series were designed following the observation that the *para* position in most of the flufenamic acid poses faces a rather large empty pocket. The idea was then to substitute at this *para* position different groups of variable lengths so as to provide additional favorable interactions with the protein. The derivative of flufenamic acid with the nitro and amino groups at the *para* position of the carboxyl group (compounds **4a** and **4b**) docked into the binding site adopts geometries again close to those of flufenamic acid. Two other poses feature a geometry shifted to CN⁻ with a correspondence of the two oxygens of the carboxylate group onto two crystal water molecules closer to CN⁻. The two oxygens of the nitro group fit onto two other crystal water molecules. The amino group in compound **4a** makes a hydrogen bond with one propionate group of the heme and with Glu102.

Compound **5** series was designed by substituting longer chains at the *para* position of flufenamic acid. The rationale behind it comes from the observation that residues with different physicochemical properties line the large pocket aforementioned and thus that longer chains, bearing different functional groups at their extremities, could interact favorably with some of these residues. Two types of geometries adopted by compounds **5** can be identified in the binding site. One class of geometries corresponds closely to the geometries of flufenamic acid, that is, most of the poses position the carboxylate group onto SCN⁻. Compounds **5a**, **5b**, and **5e** belong to this class. Compound **5c** however features a larger variety of poses than the other two. One reason might be that this molecule bears a NH₃⁺ at one extremity. In all poses, the NH₃⁺ group of the ligand forms a salt bridge with the side chain of Glu116 which seems to influence

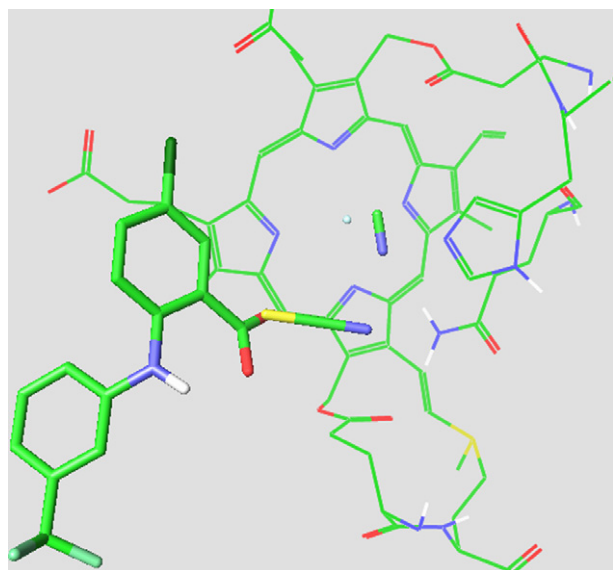


Figure 4. Best pose of compound **3c**. The ligand is depicted as sticks; neighboring residues and the heme are represented as thinner lines. The small blue sphere indicates the location of the Fe ion at the center of the heme. For sake of comparison the SCN⁻ and CN⁻ ions from the complexed structure (PDB code: 1DNW) are also shown and depicted as sticks.

the position of the benzoic acid moiety. In 5 out of 10 poses, the geometry of interaction for the carboxylate group of compound **5e** matches that of the flufenamic acid. The other class of geometries adopted by compounds **5c** and **5d** strongly differs from those of the other flufenamic acid derivatives. For compound **5d**, the OH group matches the location of the carbon of the CN^- while the carbonyl oxygen coincides with the crystal position of SCN^- in 6 out of 10 poses. Both oxygens match the locations of two crystal water molecules in the native structure. In these poses, the OH group hydrogen bonds to His95. This geometry for the OH group agrees with the location expected for H_2O_2 .¹⁸ For compound **5c**, all poses correspond to geometry with the negatively charged carboxylate of the olefinic chain matching that

of CN^- . In these geometries, the carboxylate group of the olefinic chain hydrogen bonds to Gln91 or Arg239.

2.2. Chemistry

Methods used for the synthesis of flufenamic acid derivatives (Fig. 5) were mostly based on Hartwig–Buchwald coupling reactions.¹⁹ As an example for the diacids, the synthesis of compound **2** started from 2-nitrophthalic acid (**6**, Scheme 1). Since esterification using SOCl_2 in MeOH failed,²⁰ most probably as a consequence of the presence of a nitro group, a nucleophilic substitution with MeI was carried out, which was only feasible using DBU and not weaker bases such as K_2CO_3 .²¹ After reduction of the nitro group, the aminophthalate **8**

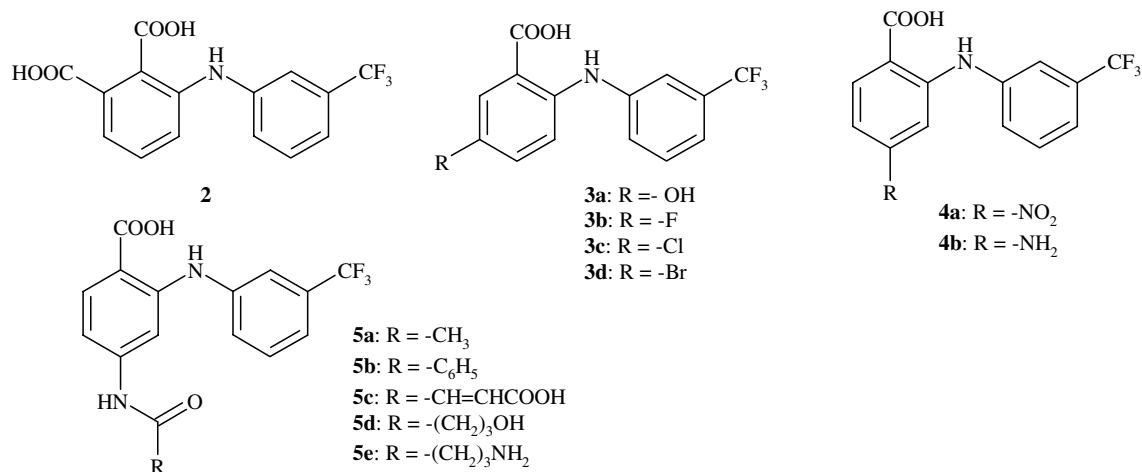
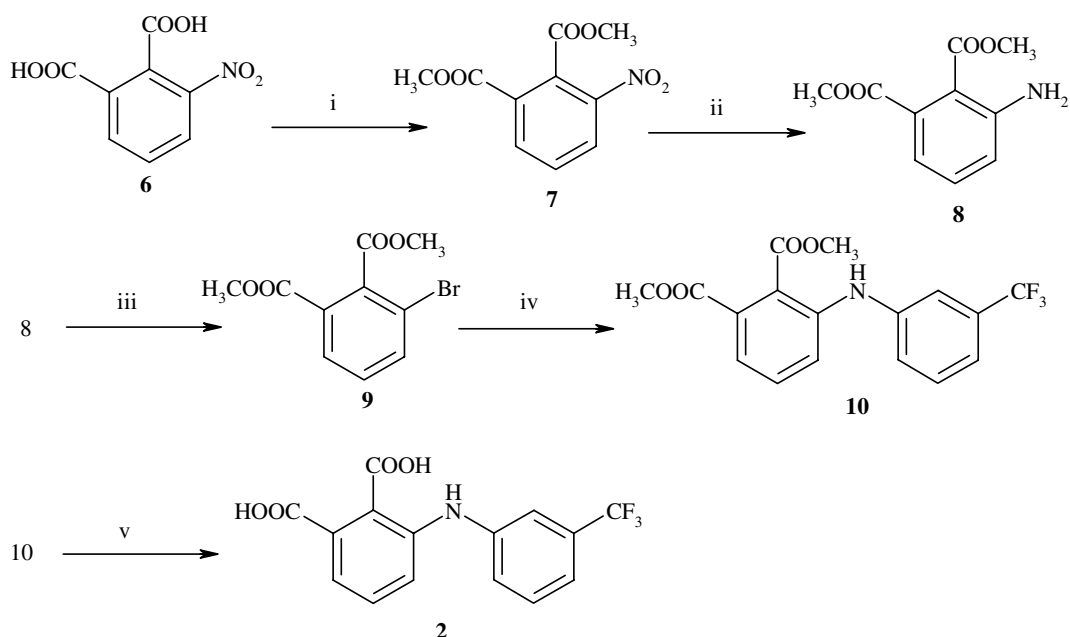


Figure 5. Structures of synthesized compounds.



Scheme 1. Synthesis of compound **2**. Reagents: (i) MeI, DBU, MeCN; (ii) H₂, Pd/C 5%; (iii) NaNO₂, HCl, CuBr; (iv) 3-trifluoromethylaniline, Pd(CH₃COO)₂, DPePhos, Cs₂CO₃; (v) KOH, EtOH, H₂O.

was subjected to a Sandmeyer reaction and transformed into the bromo derivatives **9**.^{22,23} The Hartwig–Buchwald coupling of **9** with 3-trifluoromethylaniline delivered the ester **10** which was further hydrolyzed into the phthalic acid derivative **2**.

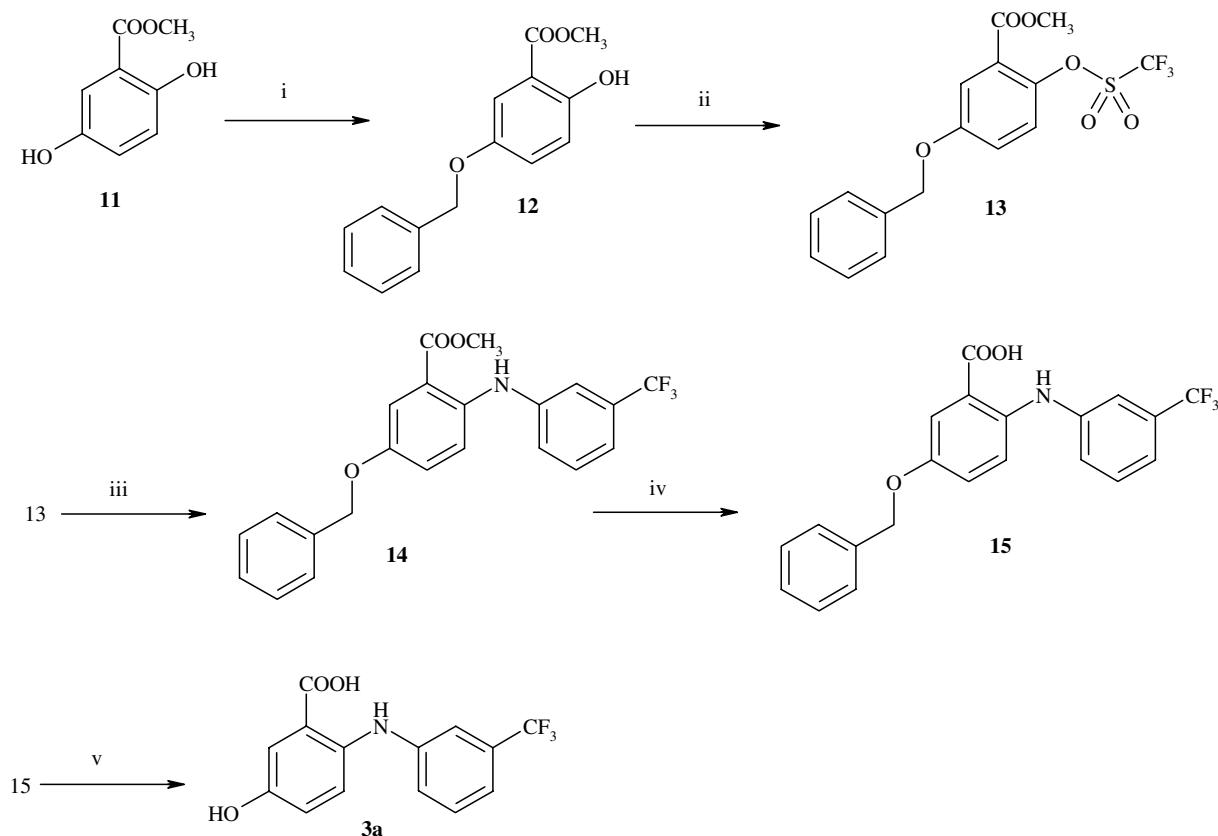
For the synthesis of compound **3a**, methyl gentisate (**11**) was used as a starting compound (Scheme 2). The first step was a regioselective protection of the phenol at position **5** by a benzyl group.²⁴ The remaining phenol was then activated by transformation into a triflate which was subjected to the Hartwig–Buchwald coupling. The ester was subsequently hydrolyzed and the benzyl protecting group removed by hydrogenolysis.²⁵ The method used for the syntheses of compounds **3b** and **3c** was similar but started from the corresponding methyl 5-halo-2-hydroxybenzoate (Scheme 3). The synthesis of 5-bromo flufenamic acid, derivative **3d**, appeared more complicated as it could not be undertaken from methyl 5-bromo-2-hydroxybenzoate (Scheme 4). Indeed, the Hartwig–Buchwald coupling with the triflate derivative gave a complex mixture of compounds which could be attributed to the higher reactivity of the bromoarenes in comparison with the corresponding chloro- and fluoroarenes. As the Sandmeyer reaction on paraphenylenediamines was not possible due to the high oxidizability of the compounds, the direct bromination of flufenamic acid with bromine was attempted using several conditions (Br₂ in acetic acid, methanol or dioxane, respectively). The best solvent appeared to be meth-

anol because acetic acid and dioxane gave higher proportions of other bromination products.

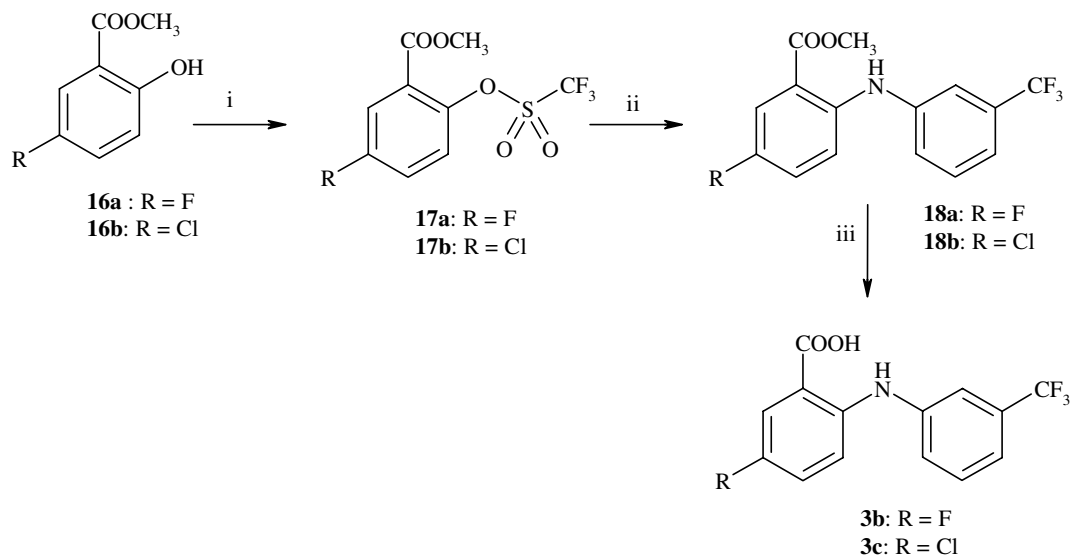
The series of flufenamic acid derivatives with substituents at position 4 of the anthranilic acid ring was obtained from a common precursor **22** (Scheme 5) with 2-bromo-4-nitrotoluene (**19**) as the starting material. After oxidation of the methyl group in a carboxylic acid,²⁶ followed by esterification via a nucleophilic substitution with MeI,²¹ a C–N coupling was carried out to obtain the nitro derivative **22**. A fraction of this compound was hydrolyzed to the acid **4a** and after a catalytic hydrogenation, the resulting amine was transformed into the amino-acid **4b**. From compound **23**, a series of five compounds was obtained. The first three include the amides **5a–c** which were prepared by amidification with the corresponding acid chlorides in a mixture of pyridine/CH₂Cl₂, followed by alkaline hydrolysis. The synthesis of compounds **5d** and **5e** was carried out from the bromo derivative **27**, either by reaction with potassium acetate and hydrolysis of both ester functions or by nucleophilic substitution with NaN₃, catalytic hydrogenation, and finally hydrolysis.

2.3. Biological activity

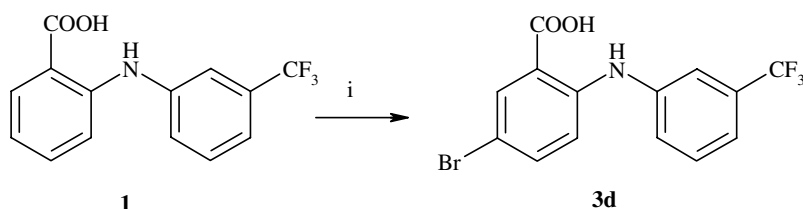
The biological activity of flufenamic acid and its analogs was first assessed by the inhibition of the chlorinating activity of MPO with the taurine assay. The amount of MPO was chosen to produce 60 μM of HOCl in



Scheme 2. Synthesis of compound **3a**. Reagents: (i) benzyl bromide, K₂CO₃, acetone; (ii) (CF₃SO₂)₂O, TEA, CH₂Cl₂; (iii) 3-trifluoromethylaniline, Pd(CH₃COO)₂, DPePhos, Cs₂CO₃; (iv) KOH, EtOH, H₂O; (v) H₂, HCl, Pd/C (5%).



Scheme 3. Synthesis of compounds **3b** and **3c**. Reagents: (i) $(\text{CF}_3\text{SO}_2)_2\text{O}$, TEA, CH_2Cl_2 ; (ii) 3-trifluoromethylaniline, $\text{Pd}(\text{CH}_3\text{COO})_2$, DPePhos, Cs_2CO_3 ; (iii) KOH, EtOH, H_2O .



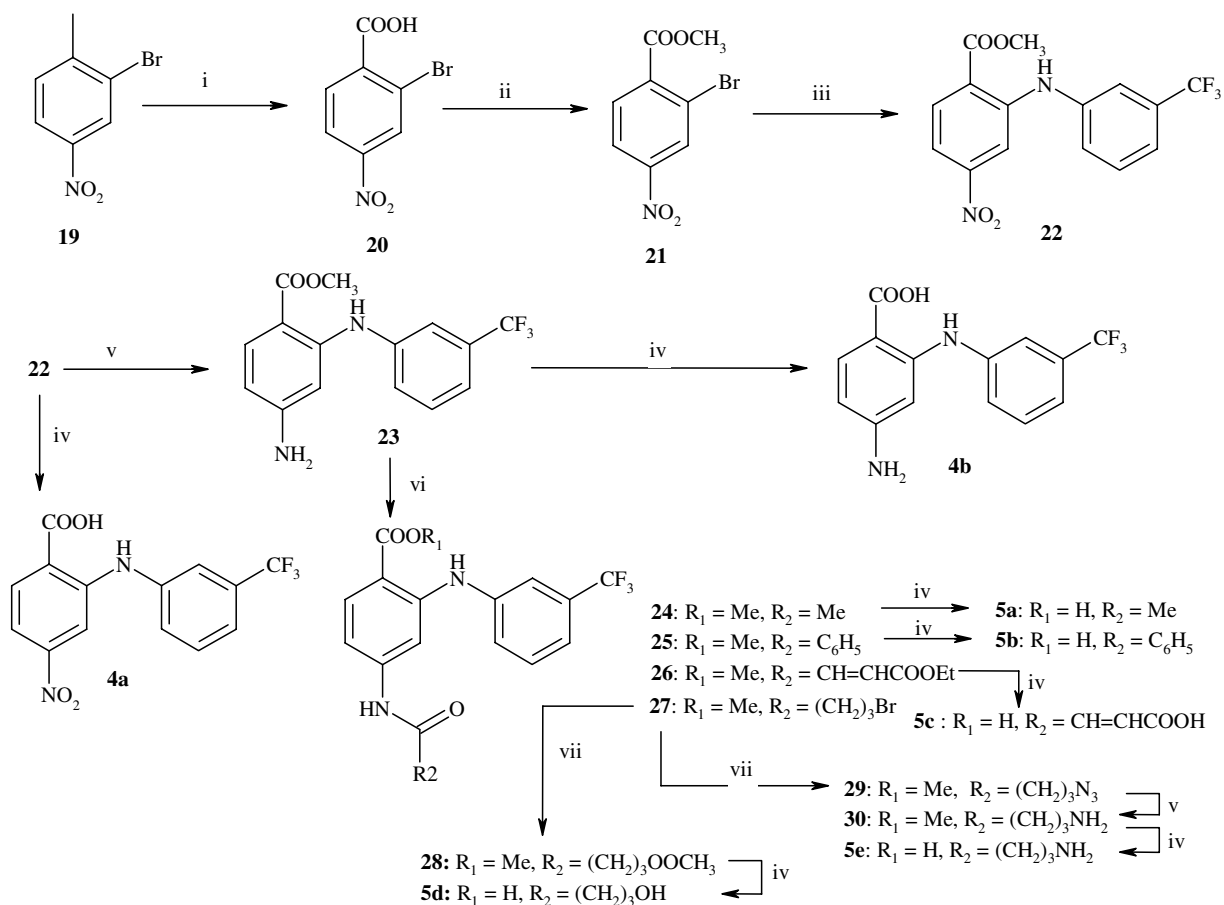
Scheme 4. Synthesis of compound **3d**. Reagents: (i) Br_2 , MeOH.

5 min at 37 °C in the presence of 100 μM of H_2O_2 and the amount of the produced taurine chloramine was measured by the thionitrobenzoic acid (TNB) reagent as previously described.^{11,12} The percentage of the inhibition was calculated taking the blank as 100% of inhibition and the chlorinating activity in absence of the compounds as the 0% of inhibition. The concentration that inhibits at least 50% (IC_{50}) of the MPO activity was calculated by establishing sigmoid curves of the MPO activity as a function of compound concentration. The curves were fitted with a three-parameter sigmoid model. The scavenging activity of compounds was simultaneously assessed by replacing the MPO system with 60 μM of HOCl and by measuring the produced taurine chloramines with the same procedure.

In the meantime, the accumulation of compound II was measured for the different compounds in the absence or the presence of chloride. Figure 6 shows that MPO, a ferric-porphyrin (Por) enzyme form ($\text{Fe}^{\text{III}} \cdot \cdot \text{Por} \cdot \cdot \text{aa}$), is oxidized by H_2O_2 to give compound I, an oxy-ferryl intermediate characterized by a structure which is deficient in two electrons ($\text{Fe}^{\text{IV}}=\text{O} \cdot \cdot \text{Por}^+ \cdot \cdot \text{aa}$), one removed from iron and one from porphyrine (Por^+). Compound I is able to produce HOCl in the presence of chloride ions (Cl^-) returning to the native enzyme state. However, in conditions such as the absence of Cl^- , the presence of an excess of H_2O_2 or the presence of a molecule able to inhibit the formation of HOCl, the system evolves to the promotion

and the accumulation of compound II, a reduced form of compound I ($\text{Fe}^{\text{IV}}=\text{O} \cdot \cdot \text{Por} \cdot \cdot \text{aa}$).^{27–30} As a consequence, the accumulation of compound II is a semi-quantitative spectral method suitable to document the inhibiting effect of the molecules by using the specific spectral patterns of MPO (λ_{max} 430 and 575 nm), compound I (λ_{max} 430 nm), and compound II (λ_{max} 456 and 625 nm). As the MPO system is relatively complex, it is of importance to classify and separate molecules acting as electron donors (AH) with the oxidized forms of the enzyme (compounds I and II) or as antagonists of chloride in the catalytic site of MPO. It is generally admitted that a molecule which rapidly converts compounds I and II into native MPO is an electron donor (AH) that quickly consumes H_2O_2 and also generates unwanted oxidized by-products during the reaction.¹² However, a molecule that rapidly reduces compound I but slowly reacts with compound II is considered as a chloride antagonist that promotes the accumulation of compound II. This last case is more suitable for therapeutic purposes as it depletes the pool of native MPO and generates less oxidation adducts during the inhibition (Fig. 6). In terms of compound II accumulation, the first molecules are characterized by a short lifetime of compound II in the absence or the presence of chloride while the second ones are characterized by a longer lifetime of compound II in both the conditions.

Finally, the inhibition of LDL oxidation was evaluated in the presence of several concentrations of the synthe-



Scheme 5. Synthesis of compounds **4a–b** and **5a–e**. Reagents: (i) KMnO_4 , pyridine; (ii) MeI, DBU, MeCN; (iii) 3-trifluoromethylaniline, $\text{Pd}(\text{CH}_3\text{COO})_2$, DPePhos, Cs_2CO_3 ; (iv) KOH, EtOH, H_2O ; (v) H_2 , Pd/C (5%), MeOH; (vi) R_2COCl , pyridine, CH_2Cl_2 ; (vii) NaN_3 or CH_3COOK , DMF.

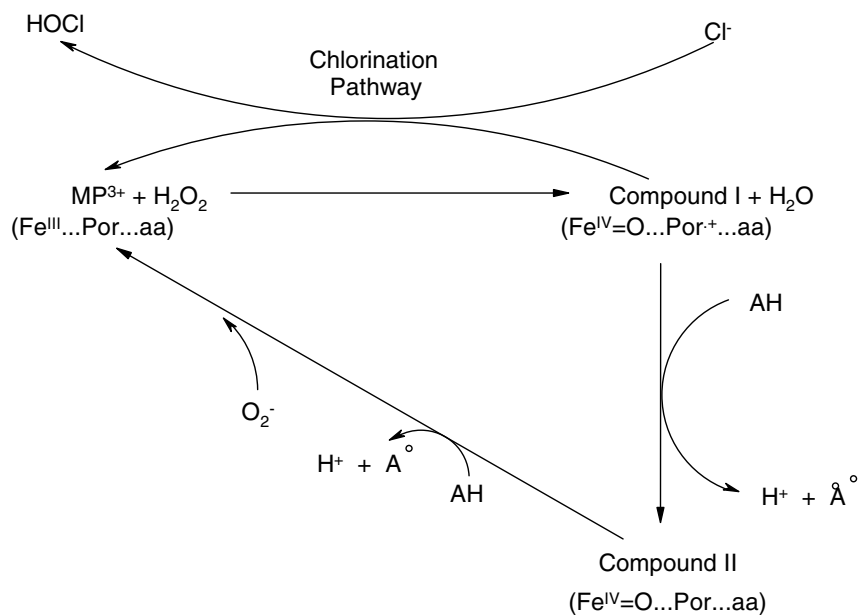


Figure 6. Representation of MPO redox transformation catalytic pathways. MP^{3+} : native enzyme; compound I: $\text{MP}^{3+} \text{H}_2\text{O}_2$; compound II: $\text{MP}^{2+} \text{H}_2\text{O}_2$; AH: reducing agent; O_2^- : superoxide anion. Adapted from Kettle and Winterbourn.³⁰

sized molecules by a recently developed ELISA.⁷ The LDL oxidation in absence of candidate inhibitors was

considered as the 100% and the native LDL as the 0%. This assessment takes into account the binding capacity

of this enzyme on negatively charged macrostructure like LDLs and actually improves the relevance of the results in a physiological context.⁶

The experimental data are summarized in Table 1 that assembles the results of the docking, the accumulation of compound II, and the inhibiting effect measured by the taurine assay. Table 2 compares the percentage of HOCl scavenging to the percentage of MPO inhibition at four relevant physiological concentrations in order to illustrate the enzyme inhibition capacity of compounds independently of their scavenging activity toward HOCl. The inhibition of LDL oxidation is illustrated in Figures 7 and 8. Except for compounds 5c and 2, the docking free energies (ΔG kcal/mol) were very close to flufenamic acid. Furthermore, a similar inhibiting effect was noted (Table 1) as far as the 5-halogenous substituted compounds (3b–d) are concerned. However, none of the synthesized molecules were able to efficiently inhibit LDL oxidation (Figs. 7 and 8) or to have an increased activity as compared to flufenamic acid.

The results with the phthalic derivatives of flufenamic acid (diacid compounds) clearly show that the addition of a carboxylic function suppresses the interaction with MPO. More interesting is the substitution of flufenamic acid on position 5. According to the docking, molecules adopt a position similar to the one of flufenamic acid. However, compound 3a (5-OH derivative) induces a pro-oxidative effect on the system, while compounds 3b–d have an activity similar to flufenamic acid without any scavenging toward HOCl. The lifetime of com-

pound II is 2.21 and 2.41 times superior to flufenamic acid with compounds 3b (5-F) and 3c (5-Cl), respectively, suggesting a reduced turn-over of native MPO by the peroxidase cycle. However, compound 3d (5-Br) has a similar interaction with the MPO/H₂O₂/Cl⁻ system as flufenamic acid. Compound 3a is characterized by the absence of compound II formation in the experimental conditions. The redox properties of this molecule that is liable to be oxidized in a quinonimine could explain this phenomenon and the probable pro-oxidant effect. Indeed, the TNB reagent used in the taurine assay could form a Michael adduct with the quinonimine form that increased the consumption of the reagent. Finally, the addition of a chemical group at position 5 causes a decreased inhibition of LDL oxidation. Flufenamic acid inhibits LDL oxidation in a dose-dependent manner but compounds 3a, 3b, and 3d only show a significant inhibition at 300 μ M (respectively, 53 \pm 8%, 9 \pm 5% and 29 \pm 5%) while no inhibition was observed with compound 3c (112 \pm 6%).

Compounds in group 4 are the precursors of the compound 5 family and again have geometries close to the one of flufenamic acid. Moreover, the 4-nitro derivative demonstrates the same inhibiting effect as flufenamic acid ($P > 0.05$, Bonferroni *t*-test) without any reactivity toward HOCl. However as demonstrated by the lifetime of compound II, this molecule deeply accumulates the compound II, depleting the amount of native MPO for the HOCl production. This molecule is considered as a real antagonist of chloride in the catalytic site. The presence of the nitro group is probably responsible for an electroattractant effect, decreasing the oxidation in posi-

Table 2. Percentages of the scavenging activity toward HOCl at relevant pharmacological concentrations in comparison to the percentages of MPO inhibition for the synthesized compounds

Compound	% of scavenging ^a /% of inhibition			
	0.5 μ M	1 μ M	2 μ M	4 μ M
Flufenamic acid	2 \pm 2	1.1 \pm 0.2	1.6 \pm 0.6	1.7 \pm 0.6
	25 \pm 8	40 \pm 2	52 \pm 2	64 \pm 1
Compound 3a (5OH ⁻)	2 \pm 1	2 \pm 1	2.5 \pm 0.1	2 \pm 1
	-70 \pm 3	-73 \pm 1	-72 \pm 1	-73 \pm 1
Compound 3b (5F ⁻)	3.3 \pm 0.7	2.0 \pm 0.5	1.9 \pm 0.5	3 \pm 1
	37 \pm 5	49 \pm 2	63 \pm 3	76 \pm 2
Compound 3c (5Cl ⁻)	1 \pm 2	0.4 \pm 0.4	2 \pm 1	1 \pm 1
	29 \pm 1	42 \pm 1	57 \pm 4	74 \pm 3
Compound 3d (5Br ⁻)	3 \pm 1	2 \pm 1	3 \pm 1	4.9 \pm 0.7
	36 \pm 1	51 \pm 1	65 \pm 2	79 \pm 1
Compound 4a	0 \pm 1	0 \pm 1	1 \pm 1	2 \pm 1
	29 \pm 2	29 \pm 2	43 \pm 3	55 \pm 2
Compound 4b	1 \pm 2	2 \pm 2	2 \pm 2	3 \pm 4
	-18 \pm 2	-28.6 \pm 0.7	-30.7 \pm 0.3	-31.5 \pm 0.1
Compound 5a	1 \pm 1	2 \pm 3	2 \pm 5	1 \pm 2
	12 \pm 2	24 \pm 8	33 \pm 7	42 \pm 2
Compound 5b	1 \pm 2	0 \pm 2	0 \pm 1	2 \pm 2
	11 \pm 2	15 \pm 1	25 \pm 2	35 \pm 2
Compound 5c	-1 \pm 1	-1 \pm 1	0 \pm 2	2 \pm 1
	0.3 \pm 0.4	0.6 \pm 0.2	0.1 \pm 0.6	0.3 \pm 0.2
Compound 5d	0 \pm 1	0 \pm 1	-1 \pm 1	1 \pm 4
	8.5 \pm 1	12 \pm 3	12.2 \pm 0.6	20 \pm 3
Compound 5e	1 \pm 3	2 \pm 4	2 \pm 1	1 \pm 1
	12 \pm 5	21 \pm 7	35 \pm 3	49 \pm 4

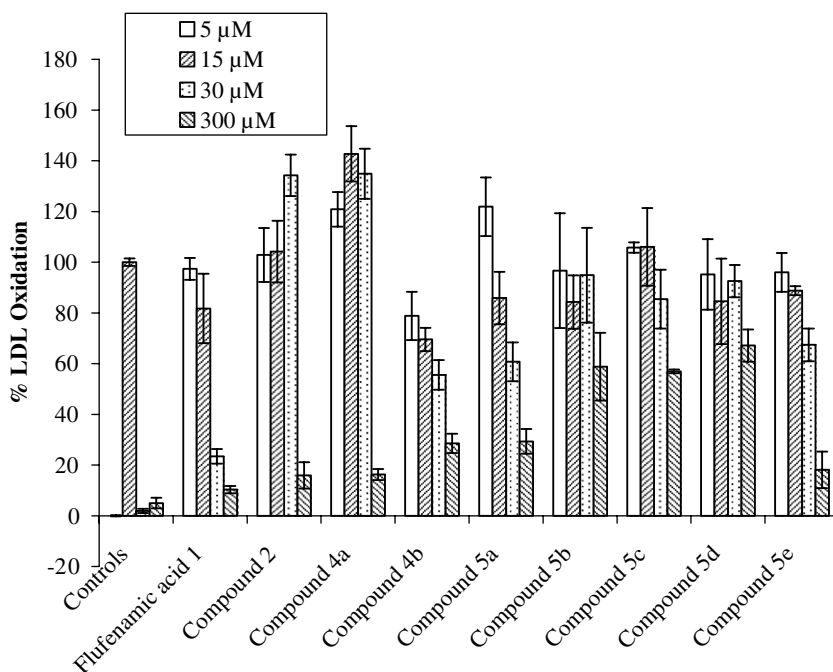


Figure 7. LDL oxidation (in %) in relation to different concentrations of flufenamic acid and analogs: 5 μM (\square), 15 μM (▨), 30 μM (▩), and 300 μM (▧). Absorbance of LDL (Blank; controls, \square) and oxidized LDL without drugs (controls, ▨) is, respectively, considered equal to the 0 and 100%. In absence of H_2O_2 , % = $2 \pm 1\%$ (controls, ▩); in presence of catalase (400 U/mL) (controls, ▧), % = $5 \pm 2\%$. Results are means \pm SD for $n = 3$. Percentages of LDL oxidation in the presence of flufenamic acid: $97 \pm 4\%$, 5 μM ; 82 ± 14 , 15 μM ; $23 \pm 3\%$, 30 μM ; $10 \pm 1\%$, 300 μM .

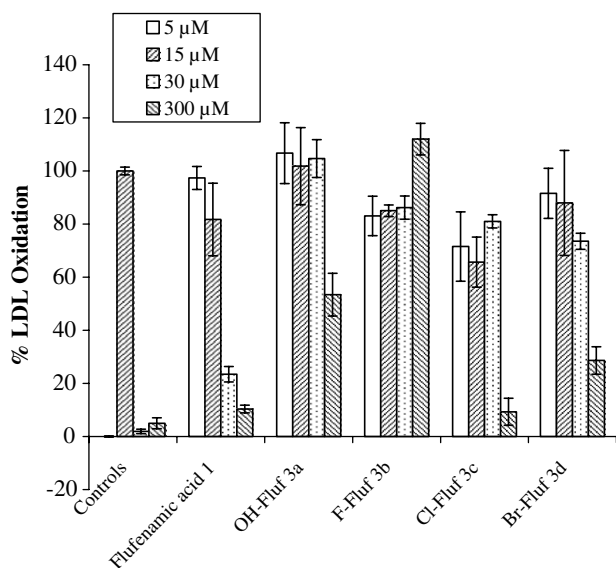


Figure 8. LDL oxidation (in %) in relation to different concentrations of flufenamic acid and analogs: 5 μM (\square), 15 μM (▨), 30 μM (▩), and 300 μM (▧). Absorbance of LDL (Blank; controls, \square) and oxidized LDL without drugs (controls, ▨) is, respectively, considered equal to the 0 and 100%. In absence of H_2O_2 , % = $2 \pm 1\%$ (controls, ▩); in presence of catalase (400 U/mL) (controls, ▧), % = $5 \pm 2\%$. Results are means \pm SD for $n = 3$. Percentages of LDL oxidation in the presence of flufenamic acid: $97 \pm 4\%$, 5 μM ; 82 ± 14 , 15 μM ; $23 \pm 3\%$, 30 μM ; $10 \pm 1\%$, 300 μM .

tion 5. Compound **4b** is the 4-amino derivative which seems to react with the $\text{MPO}/\text{H}_2\text{O}_2/\text{Cl}^-$ system in the same way of the 5-OH derivative (compound **3a**). The

addition of a chemical group in position 4, such as for compounds **3a–d**, decreases the inhibition of LDL oxidation as compared to flufenamic acid (compound **4a**: $121 \pm 7\%$, $143 \pm 11\%$, $135 \pm 10\%$, $16 \pm 2\%$). Finally, compound **4b** inhibits the oxidation in a dose-dependent manner ($79 \pm 9\%$, $70 \pm 5\%$, $56 \pm 6 \mu\text{M}$, $29 \pm 4\%$).

Compounds from series **5** include olefinic or alkyl 4-carboxamido substituted flufenamic acid derivatives. They all have a decreased activity as compared to flufenamic acid, which is related to a short lifetime of compound **II** in the presence of chloride. They also do not react with HOCl . Compound **5c** is particularly interesting: indeed, the docking procedure predicts an efficient inhibition ($\Delta G = -7.74 \text{ kcal/mol}$) which contrasted with the experimental data. The discrepancy is illustrated by the accumulation of compound **II** in which the lifetime of compound **II** is decreased in the presence of chloride and increased in its absence, illustrating a weaker interaction with the enzyme compared to flufenamic acid. Possibly another explanation lies in the mass/charge ratio (m/z), such as demonstrated by Burner et al.³¹ As a matter of fact, the catalytic site is embedded in a hydrophilic pocket accessible via a narrow oval shaped hydrophobic channel and the addition of a negative charge to the structure of the ligand could hamper an inhibition process.¹³ With the exception of compound **5c**, the other molecules of group **5** more rapidly react with compound **II** than flufenamic acid; however, this is not related to a better inhibition as they are unable to sufficiently accumulate compound **II** in presence of chloride. It is interesting to note that the interaction with compound **II** would be privileged as the 5 position is free and could be exposed to oxidation. According to the ELISA, only

compound **5a** was able to inhibit LDL oxidation in a dose-dependent manner ($122 \pm 12\%$, $86 \pm 10\%$, $61 \pm 8\%$, $29 \pm 5\%$). The addition of more voluminous chemical groups or substituents at position 4 seems to have a negative influence on the inhibiting effect.

3. Conclusions

The docking process of flufenamic acid and of its analogs in the catalytic site of the enzyme provided interesting data which helped to discriminate active molecules and to predict the efficiency of several compounds. However, the information carried out was in some cases rather limited as a consequence of the mechanistic complexity of MPO. Indeed, only a non-significant correlation coefficient of 0.63 could be derived from the curve of the percentage of inhibition plotted as a function of the predicted free energy (ΔG , excluding the prooxidant and inactive molecules). This could be attributed to the narrow range of free energy values, which are within the error value of 2 kcal/mol usually accepted for such a parameter. Moreover, MPO preferably reacts with small substrates and the enzyme is rapidly oxidized in compound I by H_2O_2 ($K_s = \sim 10^7 \text{ M}^{-1} \text{ s}^{-1}$).³² Therefore, the actual inhibitors intensively react with the peroxidase cycle of the enzyme and to different extent with compounds I and II. As a matter of fact, the reactivity of the molecules with compounds I and II cannot be predicted by a conventional docking. Moreover, the virtual procedure does not take into account the penetration of the drugs through the oval shaped hydrophobic channel which connects the catalytic site to the outer surface of the enzyme.

In spite of these limitations, the present investigation permits to draw some conclusions useful for a rational conception of MPO inhibitors. First, the mass/charge ratio is a determinant parameter to discriminate the molecules able to enter the catalytic site, such as already demonstrated by Burner et al. for thiol-containing molecules.³¹ Second, the nucleophilic properties of the molecules have to be carefully considered. Indeed, flufenamic acid, which is an efficient inhibitor of the MPO/ $\text{H}_2\text{O}_2/\text{Cl}^-$ system, acts as an electron donor. The 5-position which is free on the molecule, is favorable to a rapid oxidation by compounds I and II. A substitution at this position with a halogen slightly increases the inhibiting effect and decreases the reactivity with compound II (its lifetime in the presence of chloride increases). This statement is confirmed by the addition of a nitro group at position 4 that dramatically decreases the reaction rate with compound II by exerting an electroattractant effect on position 5. Third, the MPO inhibition is strongly dependent on the used model. This cationic enzyme is liable to be adsorbed on negatively charged macrostructures like LDLs that could modify the accessibility to the catalytic site.⁵ Moreover, a previous study demonstrated that the size of the molecule is a crucial parameter for the inhibition of MPO-dependent LDL oxidation.¹⁶ Indeed, flufenamic acid that inhibits MPO was unable to inhibit the MPO-dependent LDL oxidation contrary to small thiol-containing molecules

like *N*-acetylcystein. In this context, the addition of bigger atoms at position 5 or of small linear hydrocarbon chains at position 4 dramatically reduces the inhibition of LDL oxidation in spite of a better inhibiting effect.

The rational conception of MPO inhibitors should therefore move to molecules that better fit to these observations. For example, negatively charged molecules have been considered in a mass/charge ratio but the impact of positive charge on the inhibitor structure should be assessed. Small molecules with only one aromatic ring could also fit to the inhibition of MPO as this reduces the mass of the inhibitor and also brings about more planar structure that could properly sneak between LDL and MPO. The substitution on the aromatic ring will have to be chosen to avoid electrophil attack and the oxidation by the compound I of MPO. Finally, a virtual modeling of the channel that brings the drugs to the catalytic site would be a convenient tool to enhance the predictions. The MPO inhibition would benefit from all these careful considerations, reducing the discrepancies arising from the considered experimental models.

4. Experimental

4.1. Molecular modeling

4.1.1. Protein preparation. The X-ray structure of human MPO complexed to cyanide and thiocyanate (PDB code: 1DNW) was used as the target structure to endeavor the docking studies.¹³ The X-ray water and the CN^- and SCN^- molecules were removed from the active site.

4.1.2. Ligand preparation. The ligand input files were prepared according to the following procedure. The initial 3D structures of the ligands were generated using Corina³³ and the ligand partial charges were ascribed using the OPLS force-field as performed by Glide.

4.1.3. Docking. The Glide (Grid-Based Ligand Docking With Energetics) algorithm approximates a systematic search of positions, orientations, and conformations of the ligand in the receptor binding site using a series of hierarchical filters (www.schrodinger.com).¹⁷ The shape and properties of the receptor are represented on a grid by several different sets of force-fields that provide progressively more accurate scoring of the ligand pose. The fields are computed prior to docking. The binding site is defined by a rectangular box confining the translations of the mass center of the ligand. A set of initial ligand conformations is generated through exhaustive search of the torsional minima augmented by a heuristic approach that eliminates conformations unsuitable for binding to a receptor. The conformers are clustered in a combinatorial fashion. Each cluster, characterized by a common conformation of the core and an exhaustive set of side-chain conformations, is docked as a single object in the first stage. The search begins with a rough positioning and scoring phase that significantly narrows the search space and reduces the number of poses to be further considered to a few hundred. In the following

stage, the selected poses are minimized on precomputed OPLS-AA van der Waals and electrostatic grids for the receptor. In the final stage, the 5–10 lowest-energy poses obtained in this fashion are subjected to a Monte Carlo procedure in which nearby torsional minima are examined, and the orientation of peripheral groups of the ligand is refined. In the present work, the binding region was defined by a $18 \text{ \AA} \times 18 \text{ \AA} \times 18 \text{ \AA}$ box centered on the central position of the cyanide in the crystal complex. At the most 10 poses were generated for each molecule. Default settings were used for all the remaining parameters.

4.1.4. Evaluation of scoring. The minimized poses generated by Glide are scored using the GlideScore function (www.schrodinger.com),¹⁷ which is a more sophisticated version of the empirical ChemScore function with additional force field-based components and terms accounting for solvation and repulsive interactions.^{17,34} Contributions arise from lipophilic and hydrogen bonding interactions. Metal–ligand interactions are described by a specific term. Contributions from force-field Coulomb and van der Waals interaction energies are incorporated in the empirical-based function. Various databases of ligands were used to parameterize the coefficients of the functional form. The choice of the best pose is made using a model energy score (E_{model}) that combines the energy grid score, GlideScore, and the internal strain of the ligand.

4.2. Chemistry

Starting compounds and solvents for reactions or NMR analysis were purchased from Sigma–Aldrich. Except when indicated, compounds were not purified and solvents were not dried before use. NMR spectra (at 300 MHz for ¹H and at 75 MHz for ¹³C) were recorded on a Bruker Avance 300 at 293 K. Tetramethylsilane (TMS) was used as internal standard and δ are expressed in ppm. The IR spectra were taken on a Shimadzu IR-470 infrared spectrophotometer and ν are given in cm^{-1} . Solid compounds were dispersed in KBr (1% (m/m)) and liquid compounds were spread on a NaCl plate. Column chromatography (CC) separations were performed with Kieselgel 100[®] (Merck) and TLC analyses were carried out on Kieselgel GF₂₅₄[®] plates (Merck).

4.3. General procedure for the synthesis of esters

DBU (47.4 mmol for compound 20 and 94.8 mmol for compound 6) and MeI (94.8 mmol for acid 20 and 0.142 mol for acid 6) were added to a suspension of the acid (47.4 mmol) in acetonitrile (50 mL). The solid slowly dissolved and the solution was stirred for 16 h. The solvent was evaporated under reduced pressure and the residue was dissolved in diethyl ether (150 mL). The organic phase was washed with 2 M HCl (100 mL), 2 M NaOH (100 mL), and brine (50 mL). After drying with Na₂SO₄ and filtration, the solvent was evaporated under reduced pressure.

4.3.1. Dimethyl 3-nitrophthalate (7). Yellowish oil that slowly crystallized (64%); ¹H NMR (CDCl₃): δ 3.92 (s, 3H, OCH₃), 3.99 (s, 3H, OCH₃), 7.67 (t, $J = 8.9$ Hz,

1H, H5), 8.30 (m, 2H, H4, H6); analyses were similar to those previously published.³⁵

4.3.2. Methyl 2-bromo-4-nitrobenzoate (21). Yellow solid (99%); ¹H NMR (CDCl₃): δ 3.99 (s, 3H, OCH₃), 7.92 (d, 1H, 8.4 Hz, H6), 8.21 (dd, 1H, $J = 2.4, 8.7$ Hz, H5), 8.52 (d, $J = 2.4$ Hz, 1H, H3); analyses were similar to those of the literature.³⁶

4.4. General procedure for catalytic hydrogenation

Pd/C 5% (0.78 g) was added to a suspension of the acid (47.4 mmol) in acetonitrile (50 mL). The suspension was placed in a hydrogenation flask, connected to a Parr hydrogenation apparatus, and purged with hydrogen. The mixture was stirred at room temperature for 18 h under hydrogen (414,000 Pa). After filtration on Celite, the solvent was evaporated under reduced pressure. The products were not purified.

4.4.1. Dimethyl 3-aminophthalate (8). Yellowish oil that crystallized at 0 °C (quantitative); ¹H NMR (CDCl₃): δ 3.84 (s, 3H, OCH₃), 3.86 (s, 3H, OCH₃), 5.21 (ls, 2H, NH₂), 6.78 (dd, $J = 1, 8.3$ Hz, 1H, H4), 6.89 (dd, 1H, H6), 7.23 (t, 1H, $J = 7.5$ Hz, H5).

4.4.2. Methyl 4-amino-2-[(3-trifluoromethylphenyl)amino]benzoate (23). Yellow oil which crystallized after trituration (98%); ¹H NMR (CDCl₃): δ 3.81 (s, OCH₃, 3H), 4.02 (br, NH₂, 2H), 6.06 (dd, $J = 2.1, 8.6$ Hz, 1H, H5), 6.41 (d, $J = 2.2$ Hz, 1H, H3), 7.27 (m, 1H, H4'), 7.36 (m, 2H, ArH), 7.46 (s, 1H, H2'), 7.77 (d, $J = 8.7$ Hz, 1H, H6), 9.71 (br, 1H, NH); ¹³C NMR (CDCl₃): δ 51.4 (CH₃), 97.5 (C3), 103.4 (C1), 106 (C5), 118.6 (q, $J = 4$ Hz, C2'), 119.5 (q, $J = 4$ Hz, C4'), 124.1 (q, $J = 271$ Hz, CF₃), 125.1 (C1'), 129.8 (C6'), 131.7 (q, $J = 32$ Hz, C3'), 133.8 (C5'), 141.7 (C6), 148.8 (C2), 152.2 (C4), 168.8 (COO); IR (KBr): 3455 (N–H), 3305 (N–H), 1675 (C=O), 1632, 1602, 1572, 1522, 1468, 1362, 1268, 1169, 1114, 1068, 846, 774, 691 cm^{-1} .

4.4.3. Dimethyl 3-bromophthalate (9). A 48% (m/m) solution of HBr in water (13.5 mL), water (50 mL), and amino ester 8 (6.7 g, 32 mmol) were poured in an Erlenmeyer flask. The suspension was cooled with an ice-bath and a cold (1–5 °C) solution of NaNO₂ (2.21 g, 32 mmol) in water (10 mL) was added dropwise in 5 min. The solid dissolved and, when the solution became almost clear, the reaction mixture was placed at room temperature. Then, a solution of cuprous bromide (2.53 g, 17.6 mol) in a 48% (m/m) solution of HBr in water (3.2 mL) was added dropwise. After 16 h of stirring at room temperature, the aqueous mixture was extracted three times with diethyl ether (100 mL). The organic layers were washed with 2 M NaOH (100 mL) and brine (50 mL), dried with Na₂SO₄, filtered, and evaporated under reduced pressure. The orange oil obtained (7.85 g) was purified by CC (mobile phase: CH₂Cl₂) to afford 6.41 g of white solid (yield: 73%); ¹H NMR (CDCl₃): δ 3.81 (s, 3H, OCH₃), 3.90 (s, 3H, OCH₃), 7.26 (t, $J = 8.1$ Hz, 1H, H5), 7.67 (d, $J = 8.1$ Hz, 1H, H4), 7.89 (d, $J = 7.8$ Hz, 1H, H6); ¹³C NMR (CDCl₃) δ 52.8 (OCH₃), 120.1 (C3), 128.9 (C6),

129.2 (C1), 130.2 (C5), 136.7 (C4), 137.1 (C2), 164.6 (COO), 167.6 (COO).

4.5. General procedure for the Hartwig–Buchwald coupling

Finely powdered 3-(trifluoromethyl)aniline (1.42 g, 8.8 mmol), palladium(II) acetate (33 mg, 150 μ mol), and bis[2-(diphenylphosphino)phenyl]ether (DPEphos) (20 mg, 220 μ mol) was added in an oven-dried Shlenk-tube cooled under anhydrous N₂, equipped with a magnetic stirrer. The tube was purged with anhydrous N₂. Then the bromo or triflate derivative (7.3 mmol) and toluene (10 mL) (freshly distilled on sodium) were poured into the flask. The mixture was stirred at room temperature for 5 min. Then, Cs₂CO₃ (3.34 g, 10.3 mmol) was added, the tube was purged with anhydrous N₂, and the reaction medium was heated to 100 °C for 4 h. After cooling, the brown solution was diluted with toluene (50 mL) and washed with 2 M HCl (50 mL) and brine (50 mL). The organic layer was dried with Na₂SO₄, filtered, and evaporated under reduced pressure. The compounds were purified by CC (silica gel). The mobile phases were CH₂Cl₂ for esters **10** and **22**, and petroleum ether_{40–60}/acetone (acetone gradient 0% to 2% to 5%) for compounds **14**, **18a**, and **18b**.

4.5.1. Dimethyl 3-[(3-trifluoromethylphenyl)amino]phthalate (10). Yellow solid (91%); ¹H NMR (CDCl₃): δ 3.88 (s, 3H, OCH₃), 3.90 (s, 3H, OCH₃), 7.21 (dd, J = 1.6, 7 Hz, 1H, H4), 7.26–7.43 (m, 6H, ArH), 8.04 (br, 1H, NH); ¹³C NMR (CDCl₃): δ 52.7 (OCH₃), 52.8 (OCH₃), 116.7 (q, J = 4 Hz, C2'), 117.8 (C2), 119.2 (C6'), 119.3 (q, J = 4 Hz, C4'), 120.8 (C4), 123.2 (C2), 124 (q, J = 271 Hz, CF₃), 130.1 (C6), 131.9 (C5), 132.1 (q, J = 32 Hz, C3'), 134.2 (C1), 142 (C3), 143.6 (C1'), 168.5 (COO), 168.6 (COO); IR (KBr): 3365 (N–H), 2935, 1732 (C=O), 1704 (C=O), 1572, 1520, 1535, 1277, 1250, 1121, 1004, 870, 790, 503, 477 cm⁻¹.

4.5.2. Methyl 5-phenylmethoxy-2-[(3-trifluoromethylphenyl)amino]benzoate (14). Yellow oil which slowly crystallized (67%); ¹H NMR (CDCl₃): δ 3.90 (s, 3H, CH₃), 5.04 (s, 2H, CH₂), 7.09 (dd, J = 3, 9.1 Hz, 1H, H4), 7.29 (d, J = 9 Hz, 1H, H3), 7.33–7.46 (9H, ArH), 7.59 (d, J = 3.1 Hz, 1H, H6), 9.20 (br, 1H, NH); ¹³C NMR (CDCl₃) δ 52.2 (CH₃), 70.9 (CH₂), 114.4 (C1), 116.1 (C3), 116.4 (q, J = 4 Hz, C2'), 117.2 (C6), 118.6 (q, J = 4 Hz, C4'), 123 (C4), 124.2 (q, J = 271 Hz, CF₃), 127.7 (C2'', C6''), 128.2 (C4''), 128.7 (C3'', C5''), 130 (C5', C6'), 131.9 (q, J = 32 Hz, C3'), 137 (C1''), 140.7 (C2), 142.7 (C1'), 151.3 (C5), 168.5 (COO); IR (KBr): 3340 (v N–H), 3015, 2880, 2725, 2615, 1659 (v C=O), 1617, 1582, 1522, 1497, 1458, 1418, 1389, 1334, 1286, 1264, 1218, 1170, 1125, 1150, 1065, 923, 892, 818, 787, 728, 704 cm⁻¹.

4.5.3. Methyl 5-fluoro-2-[(3-trifluoromethylphenyl)amino]benzoate (18a). Yellowish solid (75%); ¹H NMR (CDCl₃): δ 3.93 (s, 3H, OCH₃), 7.19 (d, J = 8.9 Hz, 1H, H3), 7.15–7.44 (5H, ArH), 7.64 (dd, J = 1.9, 9.4 Hz, 1H, H6), 9.35 (br, 1H, NH); ¹³C NMR (CDCl₃): δ 52.3 (OCH₃), 114 (d, J = 7 Hz, C1),

115.8 (d, J = 8 Hz, C3), 117.6 (d, J = 22 Hz, C6), 118.4 (q, J = 4 Hz, C2'), 120.1 (q, J = 4 Hz, C4'), 120.7 (d, J = 22 Hz, C4), 123.7 (q, J = 271 Hz, CF₃), 124.4 (C6'), 130.5 (C5'), 131.8 (q, J = 32 Hz, C3'), 138.6 (d, J = 2 Hz, C2), 143.5 (C1'), 151 (d, J = 235 Hz, C5), 167.9 (d, J = 2 Hz, COO); IR (KBr): 3320 (N–H), 1692 (C=O), 1586, 1520, 1431, 1334, 1225, 1187, 1161, 1122, 1069, 981, 910, 821, 788, 697 cm⁻¹.

4.5.4. Methyl 5-chloro-2-[(3-trifluoromethylphenyl)amino]benzoate (18b). Yellow oil (82%); ¹H NMR (CDCl₃): δ 3.90 (s, 3H, OCH₃), 7.17 (d, 1H, J = 9 Hz, H3), 7.25–7.44 (5H, ArH), 7.93 (d, J = 2.7 Hz, 1H, H6), 9.53 (br, 1H, NH); ¹³C NMR (CDCl₃): δ 52.1 (OCH₃), 113.8 (C1), 115.5 (C3), 118.2 (q, J = 4 Hz, C2'), 120 (q, J = 4 Hz, C4'), 122.7 (C5), 123.8 (q, J = 271 Hz, CF₃), 124.7 (C6'), 130 (C5'), 131 (C6), 131.9 (q, J = 32 Hz, C3'), 134.1 (C4), 141.1 (C2), 145.3 (C1'), 167.7 (COO); IR (KBr): 3315 (N–H), 3060, 2940, 1691 (C=O), 1574, 1514, 1451, 1335, 1250, 1217, 1163, 1121, 969, 924, 898, 819, 790, 729, 696 cm⁻¹.

4.5.5. Methyl 4-nitro-2-[(3-trifluoromethylphenyl)amino]benzoate (22). Yellowish solid (quantitative); ¹H NMR (CDCl₃): δ 3.97 (s, 3H, OCH₃), 7.44–7.49 (m, 3H, ArH), 7.54 (m, 2H, ArH), 7.98 (d, J = 2.2 Hz, 1H, H3), 8.14 (d, J = 8.8 Hz, 1H, H6), 9.78 (br, 1H, NH); ¹³C NMR (CDCl₃): δ 52.8 (OCH₃), 108.5 (C3), 111.7 (C5), 116.6 (C1), 119.8 (q, J = 4 Hz, C2'), 121.7 (q, J = 4 Hz, C4'), 123.8 (q, J = 271 Hz, CF₃), 125.8 (C5'), 130.6 (C6'), 132.6 (q, J = 32 Hz, C3'), 133.4 (C6), 140.2 (C1'), 148.1 (C2), 151.7 (C4), 167.8 (COO); IR (KBr): 3290 (N–H), 3090, 2940, 1686 (C=O), 1599, 1527, 1442, 3129, 1218, 1178, 1121, 1091, 1065, 870, 820, 794, 734, 710, 676 cm⁻¹.

4.6. 5-Bromo-2-[(3-trifluoromethylphenyl)amino]benzoic acid (3d)

To a stirred solution of compound **1** (0.5 g, 1.8 mmol) in MeOH (15 mL) was added 100 μ l (1.8 mmol) of bromine. The reaction was checked by TLC (mobile phase: CH₂Cl₂/MeOH 9:1) and, after 1 h, water (15 mL) was added. The yellow precipitate was filtered, dried at 60 °C under vacuum (27,000 Pa), and recrystallized in acetone/petroleum ether_{40–60} (2:25) to afford a yellow solid (340 mg, 53%); ¹H NMR (DMSO-*d*₆): δ 7.16 (d, J = 9 Hz, 1H, H3), 7.31 (d, 1H), 7.47–7.54 (4H, ArH), 7.95 (d, J = 2.1 Hz, 1H, H6), 9.65 (s, 1H, NH), 13.2 (br, 1H, COOH); ¹³C NMR (DMSO-*d*₆): δ 109.2 (C5), 115.9 (C1), 116.9 (C3), 117.1 (q, J = 4 Hz, C2'), 119.3 (q, J = 4 Hz, C4'), 124.1 (q, J = 271 Hz, CF₃), 124.3 (C6'), 130.5 (q, J = 31 Hz, C3'), 130.7 (C5'), 133.9 (C6), 136.6 (C4), 141.4 (C1'), 145 (C2), 168.5 (COO); IR (KBr): 3305 (N–H), 3050, 2900, 1661 (C=O), 1571, 1513, 1429, 1339, 1241, 1157, 1120, 883, 820, 789, 696 cm⁻¹.

4.7. General procedure for the hydrolysis of esters

Water (25 mL) and KOH were added to a solution of the ester (6.6 mmol) in ethanol (25 mL), placed in a round-bottomed flask. The amount of KOH was deter-

mined by the number of ester functions to hydrolyze: 13.2 mmol for compounds **4a**, **4b**, **5a**, **5b**, **5c**, **14**, **18a**, and **18b**; 26.4 mmol for compounds **5c**, **5d**, and **10**. The mixture was refluxed for 2 h and let to cool. After evaporation of ethanol, the acid was precipitated by addition of 2 M H₂SO₄ (pH ≈ 2). For compounds **4b** and **5c**, acid was added until maximal precipitation has been obtained (pH ≈ 5–6). The solid was filtered, washed three times with water (15 mL), and dried under reduced pressure (27,000 Pa) at 80 °C.

4.7.1. 3-[(3-Trifluoromethylphenyl)amino]phthalic acid (2). Yellow solid (88%); ¹H NMR (D₂O + 1 equivalent of NaOH): δ 7.24–7.40 (m, 5H, ArH), 7.47 (t, *J* = 9 Hz, 1H, H₆).

4.7.2. 5-Fluoro-2-[(3-trifluoromethylphenyl)amino]benzoic acid (3b). White solid (80%); ¹H NMR (DMSO-*d*₆) δ 7.30–7.38 (3H, ArH), 7.41–7.53 (2H, ArH), 7.66 (dd, *J* = 1.8, 9.6 Hz 1H, H₆), 9.43 (br, 1H, NH), 13.52 (br, 1H, COOH); ¹³C NMR (DMSO-*d*₆) δ 115.6 (q, *J* = 4 Hz, C_{2'}), 116.2 (d, *J* = 7 Hz, C₁), 117 (d, *J* = 23 Hz, C₆), 117.8 (d, *J* = 7 Hz, C₃), 118.1 (q, *J* = 8 Hz, C_{4'}), 121.3 (d, *J* = 23 Hz, C₄), 122.8 (C_{6'}), 124 (q, *J* = 271 Hz, CF₃), 129.8 (q, *J* = 31 Hz, C_{3'}), 130.4 (C_{5'}), 141.7 (C₂), 142.4 (C_{1'}), 154.7 (d, *J* = 235 Hz, C₅), 168.3 (d, *J* = 2 Hz, COO); IR (KBr): 3315 (N–H), 3060 (O–H), 2900, 1661 (C=O), 1580, 1517, 1339, 1227, 1179, 1140, 1104, 819, 699 cm⁻¹.

4.7.3. 5-Chloro-2-[(3-trifluoromethylphenyl)amino]benzoic acid (3c). Yellow solid (86%); ¹H NMR (DMSO-*d*₆): δ 7.26 (d, *J* = 8.7 Hz, 1H, H₃), 7.36 (m, 1H, ArH), 7.44 (dd, *J* = 2.4, 9 Hz, 1H, H₄), 7.57 (3H, ArH), 7.85 (d, *J* = 2.4 Hz, 1H, H₆), 9.64 (s, 1H, NH), 13.4 (br, 1H, COOH); ¹³C NMR (DMSO-*d*₆): δ 115.8 (C₃), 116.7 (C₁), 117 (q, *J* = 4 Hz, C_{2'}), 119.1 (q, *J* = 4 Hz, C_{4'}), 121.9 (C_{6'}), 124 (q, *J* = 271 Hz, CF₃), 124.2 (C₅), 130.4 (q, *J* = 29 Hz, C_{3'}), 130.6 (C_{5'}), 130.8 (C₆), 133.8 (C₄), 141.5 (C_{1'}), 144.5 (C₂), 168.5 (COO); IR (KBr): 3305 (N–H), 3055 (O–H), 2905, 1654 (C=O), 1569, 1510, 1425, 1337, 1243, 1158, 1119, 883, 787, 694 cm⁻¹.

4.7.4. 4-Nitro-2-[(3-trifluoromethylphenyl)amino]benzoic acid (4a). Orange solid (77%); ¹H NMR (CDCl₃ + 10% CD₃OD): δ 7.37–7.46 (ArH, 4H), 7.49 (dd, *J* = 2.3, 8.7 Hz, 1H, H₅), 7.94 (d, *J* = 2.2 Hz, 1H, H₃), 8.14 (d, *J* = 8.7 Hz, 1H, H₆); ¹³C NMR (CDCl₃ + 10% CD₃OD): δ 108.2 (C₃), 111.6 (C₅), 117.2 (C₁), 119.5 (q, *J* = 4 Hz, C_{2'}), 121.3 (q, *J* = 4 Hz, C_{4'}), 121.3 (q, *J* = 274 Hz, CF₃), 125.4 (C_{6'}), 130.4 (C_{5'}), 132.3 (q, *J* = 29 Hz, C_{3'}), 134 (C_{6'}), 141.7 (C_{1'}), 148.9 (C₂), 151.5 (C₄), 169.4 (COO); IR (KBr): 3310 (N–H), 3045 (O–H), 2905, 1662 (C=O), 1533, 1433, 1351, 1322, 1251, 1226, 1132, 820, 797 cm⁻¹; analyses were similar to those of the literature.³⁷

4.7.5. 4-Amino-2-[(3-trifluoromethylphenyl)amino]benzoic acid (4b). Beige solid (68%); ¹H NMR (CDCl₃ + 10% CD₃OD): δ 6.05 (dd, *J* = 2.2, 8.7 Hz, 1H, H₅), 6.37 (d, *J* = 2.2 Hz, 1H, H₃), 7.20 (m, H_{6'}, 1H), 7.34 (m, 2H, ArH), 7.40 (s, 1H, ArH), 7.77 (d, *J* = 8.6 Hz, 1H, H₆);

¹³C NMR (CDCl₃ + 10% CD₃OD): δ 97.3 (C₃), 103.1 (C₁), 106 (C₅), 118.3 (q, *J* = 4 Hz, C_{2'}), 119.3 (q, *J* = 4 Hz, C_{4'}), 124 (q, *J* = 271 Hz, CF₃), 125 (C₆), 129.8 (C_{6'}), 131.2 (q, *J* = 32 Hz, C_{3'}), 134.5 (C_{5'}), 141.7 (C_{1'}), 148.9 (C₂), 152.6 (C₄), 171 (COO); IR (KBr): 3433 (N–H), 3290 (N–H), 3025 (ν O–H), 2905, 2565, 1651 (C=O), 1622, 1591, 1570, 1528, 1444, 1415, 1333, 1291, 1259, 1168, 1068, 887, 835, 789, 693 cm⁻¹.

4.7.6. 4-Acetamido-2-[(3-trifluoromethylphenyl)amino]benzoic acid (5a). Beige solid (quantitative); ¹H NMR (CDCl₃ + 10% CD₃OD): δ 2.11 (s, 3H, CH₃), 6.93 (dd, *J* = 1.2, 8.6 Hz, 1H, H₅), 7.26–7.50 (m, 4H, ArH), 7.69 (s, 1H, H₃), 7.97 (d, *J* = 8.7 Hz, 1H, H₆); ¹³C NMR (CDCl₃ + 10% CD₃OD): δ 23.8 (CH₃), 103.8 (C₃), 109.5 (C₁, C₅), 117.8 (q, *J* = 4 Hz, C_{2'}), 119.3 (q, *J* = 4 Hz, C_{4'}), 123.9 (q, *J* = 271 Hz, CF₃), 124.2 (C_{1'}), 129.7 (C_{6'}), 131.6 (q, *J* = 32 Hz, C_{3'}), 133.4 (C_{5'}), 141.4 (C₆), 143.7 (C₂), 147.6 (C₄), 170.3 (CON, COO); IR (KBr): 3280 (N–H), 3105 (O–H), 2905, 1677 (C=O), 1651, 1578, 1546, 1502, 1424, 1337, 1243, 1158, 1118, 1073, 893, 789, 691, 669 cm⁻¹.

4.7.7. 4-Benzamido-2-[(3-trifluoromethylphenyl)amino]benzoic acid (5b). Beige solid (quantitative); ¹H NMR (CDCl₃ + 10% CD₃OD): δ 7.11 (dd, *J* = 1.9, 8.7 Hz, 1H, H₅), 7.27 (d, 1H, *J* = 7.7 Hz), 7.38–7.56 (m, 6H), 7.85 (3H, ArH); 8.02 (d, *J* = 8.7 Hz, 1H, H₆); ¹³C NMR (CDCl₃ + 10% CD₃OD): δ 104.5 (C₃), 108.7 (C₅), 110.2 (C₁), 118.1 (q, *J* = 4 Hz, C_{2'}), 119.3 (q, *J* = 4 Hz, C_{4'}), 123.9 (q, *J* = 271 Hz, CF₃), 124.1 (C_{1'}), 127.3 (C_{2''}, C_{6''}), 128.4 (C_{3''}, C_{5''}), 129.8 (C_{6'}), 131.6 (q, *J* = 32 Hz, C_{3'}), 131.9 (C_{4'}), 133.4 (C_{5'}), 134.6 (C_{1''}), 141.4 (C₆), 143.7 (C₂), 147.6 (C₄), 167.3 (CON), 170.3 (COO); IR (KBr): 3305 (N–H), 3015 (O–H), 2630, 1656 (C=O), 1579, 1534, 1507, 1425, 1333, 1257, 1222, 1158, 1118, 1069, 901, 790, 704 cm⁻¹.

4.7.8. (2E)-4-[(3-Carboxy-1-oxopropenyl)amino]-2-[(3-trifluoromethylphenyl)amino]benzoic acid (5c). Orange solid (quantitative); ¹H NMR (DMSO-*d*₆): δ 6.64 (d, *J* = 15.4 Hz, 1H, CH=CHCOOH), 7.08–7.13 (2H, ArH, CH=CHCOOH), 7.38 (m, 1H, ArH), 7.58–7.5 (3H, ArH), 7.83 (s, 1H, H₃), 7.91 (d, *J* = 8.8 Hz, 1H, H₆), 9.83 (s, 1H, ArNHAr), 10.64 (s, 1H, OCNH); ¹³C NMR (DMSO-*d*₆): δ 103.9 (C₃), 109.3 (C₅), 109.9 (C₁), 117.2 (q, *J* = 4 Hz, C_{2'}), 119.0 (q, *J* = 4 Hz, C_{4'}), 124.1 (q, *J* = 271 Hz, CF₃), 124.3 (C_{1'}), 130.2 (C_{6'}), 130.4 (CH=CHCOOH), 131.3 (C_{3'}), 133.1 (C_{5'}), 136.8 (CH=CHCOOH); 141.6 (C₆), 143.6 (C₂), 146.7 (C₄), 162.2 (CON); 166.2 (CH=CHCOOH), 169.3 (ArCOOH); IR (KBr): 3300 (N–H), 3030 (O–H), 1667 (C=O), 1582 (C=O), 1536, 1504, 1413, 1328, 1247, 1223, 1154, 1114, 781, 659 cm⁻¹.

4.7.9. 4-[(4-Hydroxy-1-oxobutyl)amino]-2-[(3-trifluoromethylphenyl)amino]benzoic acid (5d). Orange solid (quantitative); ¹H NMR (DMSO-*d*₆): δ 1.69 (m, 2H, O=CCH₂CH₂CH₂OH), 2.35 (t, *J* = 7 Hz, 2H, O=CCH₂CH₂CH₂OH), 3.41 (t, *J* = 6.2 Hz, 2H, O=CCH₂CH₂CH₂OH), 7.06 (dd, *J* = 1.9, 8.7 Hz, 1H, H₅), 7.36 (m, 1H, ArH), 7.56–7.57 (3H, ArH); 7.78 (d,

$J = 1.9$ Hz, 1H, H3), 7.84 (d, $J = 8.7$ Hz, 1H, H6), 9.83 (br, 1H, O=CNH), 10.08 (s, 1H, ArNHAr); ^{13}C NMR (DMSO- d_6): δ 28.2 (O=CCH₂CH₂CH₂OH), 33.3 (O=CCH₂CH₂CH₂OH), 60.1 (O=CCH₂CH₂CH₂OH), 103.3 (C3), 108.4 (C5), 109.5 (C1), 116.8 (q, $J = 4$ Hz, C2'), 118.7 (q, $J = 4$ Hz, C4'), 124.1 (q, $J = 271$ Hz, CF₃), 124.4 (C1'), 130.1 (C6'), 130.5 (q, $J = 32$ Hz, C3'), 132.9 (C5'), 141.7 (C6), 144.5 (C2), 146.6 (C4), 169.4 (COO), 172 (CON); IR (KBr): 3425 (O–H), 3280 (N–H), 2915, 1661 (C=O), 1601, 1577, 1546, 1506, 1420, 1332, 1228, 1168, 1133, 1099, 1065, 782, 693 cm^{-1} .

4.7.10. 4-[(4-Amino-1-oxobutyl)amino]-2-[(3-trifluoromethylphenyl)amino]benzoic acid (5e). White solid (31%); ^1H NMR (DMSO- d_6 + 10% of 2 M NaOH in D₂O): δ 1.75 (m, 2H, O=CCH₂CH₂CH₂NH₂), 2.37 (t, 2H, $J = 7$ Hz, O=CCH₂CH₂CH₂NH₂), 2.68 (t, 2H, $J = 6.2$ Hz, O=CCH₂CH₂CH₂NH₂), 6.90 (dd, $J = 1.9, 8.7$ Hz, 1H, H5), 7.13 (m, 1H, ArH), 7.36–7.47 (3H, ArH); 7.77 (d, $J = 1.9$ Hz, 1H, H3), 7.85 (d, $J = 8.4$ Hz, 1H, H6); ^{13}C NMR (DMSO- d_6 + 10% of 2 M NaOH in D₂O): δ 26.3 (O=CCH₂CH₂CH₂NH₂), 33.9 (O=CCH₂CH₂CH₂NH₂), 39.7 (O=CCH₂CH₂CH₂NH₂),³⁸ 104.3 (C3), 109.2 (C5), 113.6 (C1), 116.2 (q, $J = 4$ Hz, C2'), 119.1 (q, $J = 4$ Hz, C4'), 124.1 (q, $J = 271$ Hz, CF₃), 121.1 (C6'), 130.1 (C6'), 130.5 (q, $J = 32$ Hz, C3'), 132.8 (C5'), 140.9 (C1'), 143.7 (C2), 144.3 (C4), 171.2 (COO, CON); IR (KBr): 3420 (O–H), 3265 (N–H), 3060, 1649 (C=O), 1600, 1579, 1532, 1495, 1466, 1406, 1362, 1337, 1281, 1221, 1116, 1065, 825, 790 cm^{-1} .

4.7.11. 5-Phenylmethoxy-2-[(3-trifluoromethylphenyl)amino]benzoic acid (15). Yellow solid (90%); ^1H NMR (CDCl₃): δ 5.06 (s, 2H, CH₂), 7.15 (dd, $J = 3, 9.1$ Hz, 1H, H4), 7.26–7.46 (ArH, 10H), 7.66 (d, $J = 3$ Hz, 1H, H6), 9 (bs, 1H, NH), 10.1 (bs, 1H, COOH); ^{13}C NMR (CDCl₃): δ 70.8 (CH₂), 112.6 (C6), 113.9 (C1), 116.2 (C3), 117.1 (C4), 117.4 (q, $J = 4$ Hz, C2'), 119.4 (q, $J = 4$ Hz, C4'), 124.1 (q, $J = 277$ Hz, CF₃), 123.9 (C6'), 127.7 (C2'', C6''), 128.3 (C4''), 128.8 (C3'', C5''),³⁹ 131.9 (q, $J = 32$ Hz, C3'), 136.8 (C1''), 142 (C1'), 142.2 (C2), 151.3 (C4), 173 (COO); analyses were similar to those of the literature.³⁵

4.7.12. Methyl 5-phenylmethoxy-2-hydroxybenzoate (12). Methyl gentisate (5 g, 29.7 mmol) and benzyl bromide (3.5 mL, 29.7 mmol) were added to a suspension of K₂CO₃ (16.4 g, 0.119 mol) in a mixture of CHCl₃ (160 mL) and MeOH (80 mL). The mixture was refluxed for 4 h. After cooling, the suspension was filtered and the solvents were evaporated under reduced pressure. The residue was purified by CC (mobile phase: CH₂Cl₂) to give a white solid (5.8 g, 75%); ^1H NMR (CDCl₃): δ 3.5 (s, 3H, OCH₃), 5.02 (s, 2H, CH₂), 3.94 (d, $J = 9$ Hz, 1H, H6), 7.16 (dd, $J = 3.2, 9$ Hz, 1H, H4), 7.34–7.46 (ArH, 6H), 10.41 (s, 1H, OH); ^{13}C NMR (CDCl₃): δ 52.4 (CH₃), 70.9 (CH₂), 112 (C1), 113.6 (C3), 118.6 (C6), 124.9 (C4), 127.7 (C2', C6'), 128.1 (C4'), 128.7 (C3', C5'), 136.9 (C1'), 151.2 (C2), 156.3 (C5), 170.3 (COO); IR (KBr): 3300 (O–H), 1683 (C=O), 1516, 1335, 1226, 1160, 1128, 1071, 1026, 791, 745, 696 cm^{-1} , analyses were similar to those of the literature.²⁴

4.8. General procedure for the synthesis of triflates (13), (17a), and (17b)

A stirred solution of the phenol (13.2 mmol) and triethylamine (3.7 mL, 26.4 mmol) in dry CH₂Cl₂ (100 mL) was cooled with an ice-bath. To this solution, trifluoromethanesulfonic anhydride (2.5 mL, 14.6 mmol) was added dropwise. Then, the solution was let to warm to room temperature and the reaction was carried out for 8 h. The organic phase was washed with 1 M HCl (50 mL), 2 M NaOH (25 mL), and brine (25 mL). The solution was dried with Na₂SO₄, filtered, and evaporated under reduced pressure.

4.8.1. Methyl 5-phenylmethoxy-2-[(trifluoromethyl)sulfonyl]oxy]benzoate (13). The compound was purified by CC (mobile phase = CH₂Cl₂); yellow solid (96%); ^1H NMR (CDCl₃): δ 3.96 (s, 3H, CH₃), 5.10 (s, 2H, CH₂), 7.16 (dd, $J = 3, 9.1$ Hz, 1H, H4); 7.22 (d, $J = 9.1$ Hz, 1H, H3), 7.34–7.42 (m, 5H, ArH), 7.67 (d, $J = 3$ Hz, 1H, H6); ^{13}C NMR (CDCl₃): δ 52.8 (CH₃), 70.9 (CH₂), 117.8 (C1), 118.8 (CF₃, $J = 319$ Hz), 120.6 (C3), 124 (C6), 125.3 (C4), 127.7 (C2', C6'), 128.5 (C4'), 128.9 (C3', C5'), 135.8 (C1'), 141.9 (C2), 158 (C5), 164.2 (COO).

4.8.2. Methyl 5-fluoro-2-[(trifluoromethyl)sulfonyl]oxy]benzoate (17a). The product was not purified and used directly in the next step. Reddish oil; IR (KBr): 3188, 3070, 2940, 1735 (C=O), 1685, 1488, 1421 (S=O), 1300, 1272, 1241, 1205 (S=O), 1140, 1068, 901, 865, 832, 770 cm^{-1} .

4.8.3. Methyl 5-chloro-2-[(trifluoromethyl)sulfonyl]oxy]benzoate (17b). The product was not purified and used directly in the next step. Yellow oil; IR (KBr): 3085, 2940, 1732 (C=O), 1478, 1425 (S=O), 1285, 1260, 1205 (S=O), 1134, 969, 895, 846, 782 cm^{-1} .

4.8.4. 5-Hydroxy-2-[(3-trifluoromethylphenyl)amino]benzoic acid (3a). A solution of compound 15 (630 mg, 1.6 mmol) in MeOH (35 mL) was poured into a hydrogenation flask. Then, 5% Pd/C (0.1 g) and 12 M HCl (0.15 mL 1.8 mmol) were added. The flask was connected to a Parr hydrogenation apparatus and filled with hydrogen (400,000 Pa). The reaction was carried out at room temperature for 12 h. The suspension was filtered on Celite and MeOH was evaporated under reduced pressure. The solid obtained was recrystallized in ethyl acetate/petroleum ether_{40–60} (5:15) to yield yellow crystals (340 mg, 70%); ^1H NMR (CDCl₃ + 10% CD₃OD): δ 6.99 (dd, $J = 2.9, 8.9$ Hz, 1H, H7), 7.16–7.39 (ArH, 5H), 7.5 (d, $J = 2.9$ Hz, 1H, H6); ^{13}C NMR (CDCl₃ + 10% CD₃OD): δ 115.5 (q, $J = 3$ Hz, C2'), 115.5 (C6), 117.5 (C3), 117.8 (C4), 117.8 (q, $J = 4$ Hz, C4'), 122.1 (C1), 122.4 (C6'), 124.1 (q, $J = 271$ Hz, CF₃), 129.8 (C5'), 131.6 (q, $J = 32$ Hz, C3'), 139.2 (C2), 143.2 (C1'), 149.3 (C5), 170.3 (COO); IR ν 3330 (N–H), 3050 (ν O–H), 1711 (C=O), 1667, 1587, 1528, 1459, 1432, 1335, 1273, 1247, 1212, 1114, 921, 820, 785 cm^{-1} ; analyses were similar to those of the literature.³⁵

4.8.5. 2-Bromo-4-nitrobenzoic acid (20). Nitro compound 19 (24.4 g, 0.113 mol), pyridine (120 mL), and water (240 mL) were poured in a round-bottomed flask

equipped with a magnetic stirrer and a refluxed condenser. The suspension was heated to 100 °C, then removed from the oil bath and KMnO_4 (98.2 g, 0.62 mol) was added carefully in small portions.⁴⁰ The reaction was thereby maintained at reflux temperature by addition of the reagent. When addition was complete, the mixture was stirred until the temperature reached 60–70 °C. Then heating was carried out at 100 °C for 5 h. The flask was removed from the oil bath and KMnO_4 (26.8 g, 0.17 mol) was added in small portions as described above. After 16 h of stirring at 100 °C and cooling to room temperature, 13 M NaOH (15 mL) was added and the resulting suspension was filtered on Celite. The solution was washed with diethyl ether (100 mL) and then acidified to pH ~ 1 with 12 M HCl. The yellow suspension was extracted two times with diethyl ether (150 mL). The organic phase was washed with brine (50 mL), dried with Na_2SO_4 , filtered, and evaporated under reduced pressure to afford a yellowish solid (19.35 g, 70%). Analyses were similar to those of the literature.²⁶

4.9. General procedure for synthesis of amides

Amine **23** (1.2 mmol) was dissolved in a mixture of dry CH_2Cl_2 (5 mL) and TEA (1.2 mmol). The solution was cooled with an ice-bath and the corresponding acyl chloride (1.35 mmol) was added dropwise. The ice-bath was removed and the reaction was carried out at room temperature for 10 h. Then, the solution was washed with 2 M HCl (40 mL), a 10% (w/v) solution of Na_2CO_3 (40 mL), and brine (25 mL). After drying with Na_2SO_4 and filtration, the solvent was evaporated under reduced pressure. Compounds **24** and **17** were purified by CC (mobile phase: CH_2Cl_2). Amides **25** and **26** were recrystallized, respectively, in diethyl ether/hexane (1:4) and MeOH.

4.9.1. Methyl 4-acetamido-2-[(3-trifluoromethylphenyl)amino]benzoate (24). White solid (35%); ^1H NMR (CDCl_3): δ 2.06 (s, 3H, $\text{O}=\text{CCH}_3$), 3.87 (s, 3H, OCH_3), 6.89 (dd, $J = 1.7, 8.7$ Hz, 1H, H5), 7.17 (d, $J = 7.5$ Hz, 1H, ArH), 7.30 (t, $J = 7.7$ Hz, 1H, H5'), 7.38 (d, $J = 8.4$ Hz, 1H, ArH), 7.42 (s, 1H, ArH), 7.59 (s, 1H, ArH), 7.87 (d, $J = 8.8$ Hz, 1H, H6), 8.46 (br, 1H, CONH), 9.66 (s, 1H, ArNHAr); ^{13}C NMR (CDCl_3) δ 24.5 (CH_3), 51.4 (OCH_3), 103.7 (C3), 108.4 (C5), 109.6 (C1), 118.2 (q, $J = 4$ Hz, C2'), 119.6 (q, $J = 4$ Hz, C4'), 124 (q, $J = 271$ Hz, CF_3), 124.5 (C1'), 129.8 (C6'), 131.6 (q, $J = 32$ Hz, C3'), 132.9 (C5'), 141.3 (C6), 143.5 (C2), 147.7 (C4), 168.5 (COO), 169.5 (CON); IR (KBr): 3275 (N–H), 1684 (C=O), 1602, 1545, 1504, 1426, 1336, 1255, 1226, 1161, 1122, 1090, 1067, 880, 780, 694 cm^{-1} .

4.9.2. Methyl 4-benzamido-2-[(3-trifluoromethylphenyl)amino]benzoate (25). Slightly orange solid (78%); ^1H NMR ($\text{CDCl}_3 + 10\% \text{CD}_3\text{OD}$): δ 3.89 (s, 3H, OCH_3), 7.02 (dd, $J = 2.1, 8.7$ Hz, 1H, H5), 7.26 (d, $J = 6.3$ Hz, 1H, ArH), 7.37–7.53 (m, 6H, ArH), 7.71 (d, $J = 2$ Hz, 1H, H3); 7.7 (d, $J = 7.1$ Hz, 2H, H2'', H6''), 7.95 (d, $J = 8.8$ Hz, 1H, H6), 8.02 (br, 1H, CONH), 9.72 (s, 1H, ArNHAr); ^{13}C NMR ($\text{CDCl}_3 + 10\% \text{CD}_3\text{OD}$): δ 51.9 (OCH_3), 104.1 (C3), 108.7 (C5), 109.9 (C1), 118.7

(q, $J = 4$ Hz, C2'), 119.9 (q, $J = 4$ Hz, C4'), 124.1 (q, $J = 271$ Hz, CF_3), 124.8 (C1'), 127.2 (C2'', C6''), 128.9 (C3'', C5''), 130 (C6'), 132 (q, $J = 32$ Hz, C3'), 132.2 (C4''), 133.1 (C5'), 134.6 (C1''), 141.3 (C6), 143.4 (C2), 148 (C4), 166.1 (CON), 168.5 (COO); IR (KBr): 3295 (N–H), 1680 (C=O), 1645, 1620, 1589, 1507, 1424, 1235, 1150, 1113, 1081, 770, 709, 687 cm^{-1} .

4.9.3. Methyl (2E)-4-[(4-ethoxy-1,4-dioxo-2-butenyl)amino]-2-[(3-trifluoromethylphenyl)amino]benzoate (26). Yellow solid (79%); ^1H NMR ($\text{DMSO}-d_6$): δ 1.25 (t, $J = 7.1$ Hz, 3H, CH_2CH_3), 3.83 (s, 3H, OCH_3), 4.20 (q, $J = 7$ Hz, 2H, CH_2), 6.67 (d, $J = 15.5$ Hz, 1H, $\text{CH}=\text{CHCOOEt}$), 7.14–7.15 (m, 2H, H5, $\text{CH}=\text{CHCOOEt}$), 7.39 (m, 1H, ArH), 7.57–7.58 (m, 3H, ArH), 7.80 (d, $J = 1.7$ Hz, 1H, H3), 7.89 (d, $J = 8.8$ Hz, 1H, H6), 9.48 (s, 1H, ArNHAr), 10.69 (s, 1H, CONH); ^{13}C NMR ($\text{DMSO}-d_6$) δ 14 (CH_2CH_3), 51.9 (OCH_3), 60.9 (CH_2), 104.2 (C3), 108.9 (C5), 110.1 (C1), 117.3 (q, $J = 4$ Hz, C2'), 119.1 (q, $J = 4$ Hz, C4'), 124 (q, $J = 271$ Hz, CF_3), 124.4 (C6), 130 (C6'), 130.6 ($\text{CH}=\text{CHCOOEt}$), 131.6 (C3'),⁴¹ 132.6 (C5'), 137.2 ($\text{CH}=\text{CHCOOEt}$), 141.6 (C1'), 143.8 (C2), 146.4 (C4), 161.9 ($\text{O}=\text{CN}$), 164.8 ($\text{CH}=\text{CHCOOEt}$), 167.3 (ArCOOH); IR (KBr): 3325 (N–H), 1707 (C=O), 1668 (C=O), 1604, 1545, 1509, 1427, 1335, 1296, 1264, 1189, 1157, 1122, 1066, 1027, 969, 867, 794, 687 cm^{-1} .

4.9.4. Methyl 4-[(4-bromo-1-oxobutyl)amino]-2-[(3-trifluoromethylphenyl)amino]benzoate (27). Light brown solid (96%); ^1H NMR (CDCl_3): δ 2.21 (m, 2H, $\text{CH}_2\text{CH}_2\text{CH}_2\text{Br}$), 2.52 (t, $J = 7$ Hz, 2H, $\text{CH}_2\text{CH}_2\text{CH}_2\text{Br}$), 3.47 (t, $J = 6.2$ Hz, 2H, $\text{CH}_2\text{CH}_2\text{CH}_2\text{Br}$), 3.89 (s, 3H, OCH_3), 6.89 (dd, $J = 2, 8.8$ Hz, 1H, H5), 7.28 (m, 1H, ArH), 7.39–7.50 (m, 4H, ArH), 7.55 (d, $J = 1.7$ Hz, 1H, H3), 7.92 (d, $J = 8.7$ Hz, 1H, H6), 9.70 (s, 1H, ArNHAr); ^{13}C NMR (CDCl_3): δ 27.8 ($\text{CH}_2\text{CH}_2\text{CH}_2\text{Br}$), 33.3 ($\text{CH}_2\text{CH}_2\text{CH}_2\text{Br}$), 33.6 ($\text{CH}_2\text{CH}_2\text{CH}_2\text{Br}$), 51.9 (OCH_3), 103.7 (C3), 108.6 (C5), 109.5 (C1), 118.6 (q, $J = 4$ Hz, C2'), 120 (q, $J = 4$ Hz, C4'), 124.1 (q, $J = 271$ Hz, CF_3), 124.8 (C6), 130 (C6'), 131.9 (q, $J = 32$ Hz, C3'), 133.1 (C5'), 141.3 (C1'), 143.1 (C2), 147.9 (C4), 168.5 (COO), 170.3 (CON); IR (KBr): 3285 (N–H), 1675 (C=O), 1617, 1586, 1545, 1509, 1414, 1335, 1262, 1224, 1150, 1117, 1095, 780, 697 cm^{-1} .

4.10. General procedure for the nucleophilic substitutions on compound 27

The bromoalkane **27** (1.1 mmol) was dissolved in DMF (5 mL) and the nucleophile (NaN_3 or potassium acetate, 3.3 mmol) was added. The suspension was stirred overnight. Then, 50 mL of water was added and the mixture was extracted two times with toluene (50 mL). The organic solution was washed with brine (50 mL), dried with Na_2SO_4 , filtered, and evaporated under reduced pressure. The solid obtained was recrystallized in diethyl ether/petroleum ether_{40–60} (1:1).

4.10.1. Methyl 4-[(4-acetoxy-1-oxobutyl)amino]-2-[(3-trifluoromethylphenyl)amino]benzoate (28). White solid (63%); ^1H NMR ($\text{DMSO}-d_6$): δ 1.85 (m, 2H, $\text{CH}_2\text{CH}_2\text{CH}_2\text{OOCMe}$), 1.97 (s, 3H, CH_3COO), 2.38 (t,

$J = 7.5$ Hz, 2H, $\text{CH}_2\text{CH}_2\text{CH}_2\text{OOCMe}$), 3.82 (s, 3H, OCH_3), 4.01 (t, $J = 6.4$ Hz, 2H, $\text{CH}_2\text{CH}_2\text{CH}_2\text{OOCMe}$), 7.09 (dd, $J = 1.9, 8.8$ Hz, 1H, H5), 7.37 (m, 1H, ArH), 7.54–7.57 (m, 3H, ArH); 7.75 (d, $J = 1.9$ Hz, 1H, H3), 7.86 (d, $J = 8.8$ Hz, 1H, H6), 9.46 (s, 1H, ArNHAr), 10.14 (s, 1H, CONH); ^{13}C NMR ($\text{DMSO}-d_6$): δ 20.7 ($\text{CH}_2\text{CH}_2\text{CH}_2\text{OOCMe}$), 23.9 ($\text{CH}_2\text{CH}_2\text{CH}_2\text{OOCMe}$), 33 ($\text{CH}_2\text{CH}_2\text{CH}_2\text{OOCMe}$), 51.8 (OCH_3), 63.3 (CH_3COO), 103.7 (C3), 108 (C5), 109.8 (C1), 117 (q, $J = 4$ Hz, C2'), 118.9 (q, $J = 4$ Hz, C4'), 124.1 (q, $J = 271$ Hz, CF_3), 124.2 (C6), 130.5 (C6'), 131.9 (q, $J = 32$ Hz, C3'), 132.4 (C5'), 141.7 (C1'), 144.6 (C2), 146.3 (C4), 167.4 (ArCOO), 170.3 (CON), 171.3 (MeCOO); IR (KBr): 3340 (N–H), 1706 (C=O), 1676 (C=O), 1605, 1551, 1509, 1445, 1424, 1403, 1349, 1271, 1206, 1164, 1130, 1096, 1067, 1039, 869, 794, 696 cm^{-1} .

4.10.2. Methyl 4-[(4-azido-1-oxobutyl)amino]-2-[(3-trifluoromethylphenyl)amino]benzoate (29). White solid (quantitative); ^1H NMR (CDCl_3): δ 1.95 (m, 2H, $\text{CH}_2\text{CH}_2\text{CH}_2\text{N}_3$), 2.42 (t, $J = 7.1$ Hz, 2H, $\text{CH}_2\text{CH}_2\text{CH}_2\text{N}_3$), 3.37 (t, $J = 6.4$ Hz, 2H, $\text{CH}_2\text{CH}_2\text{CH}_2\text{N}_3$), 3.89 (s, 3H, OCH_3), 6.89 (dd, $J = 2, 8.7$ Hz, 1H, H5), 7.28 (m, 1H, ArH), 7.39–7.46 (m, 4H, ArH), 7.54 (d, $J = 1.7$ Hz, 1H, H3), 7.93 (d, $J = 8.8$ Hz, 1H, H6), 9.70 (s, 1H, ArNHAr); ^{13}C NMR (CDCl_3): δ 24.5 ($\text{CH}_2\text{CH}_2\text{CH}_2\text{N}_3$), 34.3 ($\text{CH}_2\text{CH}_2\text{CH}_2\text{N}_3$), 50.7 ($\text{CH}_2\text{CH}_2\text{CH}_2\text{N}_3$), 51.9 (OCH_3), 103.7 (C3), 108.6 (C5), 109.5 (C1), 118.6 (q, $J = 4$ Hz, C2'), 120 (q, $J = 4$ Hz, C4'), 124.1 (q, $J = 271$ Hz, CF_3), 124.8 (C6), 130 (C6'), 131.9 (q, $J = 32$ Hz, C3'), 133.2 (C5'), 141.3 (C1'), 143.1 (C2), 147.9 (C4), 168.5 (COO), 170.5 (CON); IR (KBr): 3285 (N–H), 2090 (N_3), 1675 (C=O), 1652 (C=O), 1617, 1583, 1546, 1509, 1439, 1414, 1349, 1261, 1222, 1165, 1115, 857, 801, 778, 698 cm^{-1} .

4.10.3. Methyl 4-[(4-amino-1-oxobutyl)amino]-2-[(3-trifluoromethylphenyl)amino]benzoate (30). Compound 29 (830 mg, 2 mmol) was dissolved in MeOH (35 mL), and 12 M HCl (0.16 mL, 2 mmol) and 5% Pd/C (0.1 g) were added. The flask was connected to a Parr hydrogenation apparatus and purged with hydrogen. The reaction was carried out for 8 h under hydrogen (400,000 kPa). Then the suspension was filtered on Celite and the solvent evaporated under reduced pressure. The residue was dissolved in water (50 mL) and this solution was made alkaline (pH \sim 14) with a 30% (w/v) solution of NaOH. After two extractions with CH_2Cl_2 (75 mL), the organic phase was washed with brine (50 mL), dried with Na_2SO_4 , filtered, and evaporated under reduced pressure. A yellow and viscous oil was obtained (720 mg, 93%). The product was not purified; ^1H NMR (CDCl_3): δ 1.62 (br, 2H, NH_2), 1.80 (m, 2H, $\text{CH}_2\text{CH}_2\text{CH}_2\text{NH}_2$), 2.45 (t, $J = 7$ Hz, 2H, $\text{CH}_2\text{CH}_2\text{CH}_2\text{NH}_2$), 2.81 (t, $J = 6.2$ Hz, 2H, $\text{CH}_2\text{CH}_2\text{CH}_2\text{NH}_2$), 3.88 (s, 3H, OCH_3), 6.98 (dd, $J = 1.9, 8.7$ Hz, 1H, H5), 7.26 (m, 1H, ArH), 7.39–7.78 (m, 3H, ArH); 7.58 (d, $J = 1.9$ Hz, 1H, H3), 7.91 (d, $J = 8.7$ Hz, 1H, H6), 9.54 (br, 1H, CONH), 9.72 (s, 1H, ArNHAr); ^{13}C NMR (CDCl_3): δ 27.9 ($\text{CH}_2\text{CH}_2\text{CH}_2\text{NH}_2$), 36.3 ($\text{CH}_2\text{CH}_2\text{CH}_2\text{NH}_2$), 41.4 ($\text{CH}_2\text{CH}_2\text{CH}_2\text{NH}_2$), 51.9 (OCH_3), 103.5 (C3), 108.2 (C5), 109.6 (C1), 118.1 (q, $J = 4$ Hz, C2'), 119.6 (q, $J = 4$ Hz, C4'), 124.1 (q, $J = 271$ Hz, CF_3),

124.6 (C6), 130 (C6'), 131.7 (q, $J = 32$ Hz, C3'), 133 (C5'), 141.5 (C1'), 144.1 (C2), 147.7 (C4), 168.6 (COO), 172.2 (CON); IR (KBr): 3290 (N–H), 2925, 1692 (C=O), 1599, 1532, 1504, 1420, 1324, 1243, 1154, 1116, 1084, 772, 695 cm^{-1} .

4.11. Methods for measurement of the biological activity

4.11.1. Preparation of solutions for the different assays. Hydrogen peroxide (H_2O_2), KI, HCl, NaCl, KOH, KH_2PO_4 , $\text{EDTANa}_2\text{H}_2$, $\text{MgCl}_2 \cdot 6\text{H}_2\text{O}$, NaHCO_3 , diethanolamine, polysorbate 80, and NaOH were obtained from VWR (Leuven, Belgium). Bovine serum albumin (BSA), 5,5'-dithio-bis-nitrobenzoic acid (DTNB), NaN_3 , paranitrophenyl phosphate, Tris(hydroxymethyl)aminomethane (Tris), methionine, and catalase were purchased from Sigma (St. Louis, USA). Sodium hypochlorite (NaOCl) was obtained from Acros Organics (New Jersey, USA).

A PBS buffer (pH 7.4) was prepared at a final concentration of 10 mM phosphate ions ($\text{KH}_2\text{PO}_4/\text{KOH}$) and 150 mM NaCl. The same phosphate buffer (pH 7.4) was also prepared without NaCl. For LDL preparation and oxidation, a PBS buffer at pH 7.2 was prepared with a final concentration of 2.8 mM of $\text{EDTANa}_2\text{H}_2$. A pH 7.5 Tris buffer saline (TBS 80) containing 50 mM of Tris, 300 mM of NaCl, and 0.1% of polysorbate 80 was used during the ELISA. Finally, a pH 9.8 diethanolamine buffer was extemporarily made up by dissolving 0.101 g of $\text{MgCl}_2 \cdot 6\text{H}_2\text{O}$ and 0.2 g of NaN_3 in water with 97 mL of diethanolamine. The pH was adjusted to 9.8 with HCl and the solution was diluted to 11. These chemicals were of pro-analysis quality. A stock solution of H_2O_2 (30% w/w) was prepared and kept at 4 °C. Before use, a working solution was prepared by dilution (60 $\mu\text{L}/50\text{ mL}$ water) and the concentration was measured using an extinction coefficient of $43.6\text{ M}^{-1}\text{ cm}^{-1}$ at 240 nm.⁴² A stock solution of NaOCl (13% w/w) was prepared and kept at 4 °C. Before use, a working solution was prepared by dilution (60 $\mu\text{L}/50\text{ mL}$ water) and HOCl concentration was determined at pH 6.2 by iodometry with a 20 mM KI solution. Iodine formed was measured at 350 nm and the concentration determined using an extinction coefficient of $22,900\text{ M}^{-1}\text{ cm}^{-1}$.⁴³ A solution of 2-nitro-5-thiobenzoate (TNB) was prepared daily as previously described and diluted to 0.45 mM after the concentration was determined using an extinction coefficient of $13,600\text{ M}^{-1}\text{ cm}^{-1}$ at 412 nm.⁴⁴ A phosphate buffer (pH 7.4), containing a final concentration of 10 mM phosphate ions ($\text{KH}_2\text{PO}_4/\text{KOH}$) and 0 or 300 mM NaCl, and an acetate buffer (pH 3.0), containing 5.0% v/v acetic acid and 0.20% m/v ammonium acetate, were prepared. De-oxygenated milli-Q water served for the preparation of all solutions.

4.11.2. Preparation of the recombinant enzyme and obtaining of LDL. Recombinant MPO was prepared as previously described.⁴⁵ Each batch of solution is characterized by its protein concentration (mg/mL), its activity (U/mL), and its specific activity (U/mg). The chlorination activity was determined according to Hewson and Hager.⁴⁶ Human plasma served for the isolation of

LDL by ultracentrifugation according to Havel et al.⁴⁷ Before oxidation, the LDL fraction ($1.019 < d < 1.067$ g/mL) was desalted by two consecutive passages through PD10 gel-filtration columns (Amersham Biosciences, The Netherlands) using PBS buffer. The different steps were carried out in the dark and the protein concentration was measured by the Lowry assay for both MPO and LDL.⁴⁸

4.11.3. Inhibition of myeloperoxidase-chlorinating activity.

The measurement of the inhibition of MPO-chlorinating activity was performed as previously described.¹² The method quantifies the amount of taurine chloramine produced by the MPO/H₂O₂/Cl⁻ system in the presence of several concentrations of compounds. The reaction mixture contained the following reagents, at the concentrations stated between brackets, in a final volume of 1.0 mL: 5 µl of recombinant myeloperoxidase (~25 nM), pH 7.4 phosphate buffer (PO₄³⁻ 10 mM/NaCl 300 mM), taurine (15 mM), and flufenamic acid analogs (0–20 µM). When necessary, the volume was adjusted to 1.0 mL with water. The mixture was incubated at 37 °C and the reaction was initiated by the addition of H₂O₂ (100 µM). After 5 min, the reaction was stopped by the addition of 100 µl of catalase (4 U/µl). Finally, the quantity of taurine chloramine was measured by the addition of 750 µl of 0.45 mM TNB and 2150 µl of water. The results were expressed as means ± SD for at least 3 different determinations for each examined drug and by taking the absence of inhibitor as the 0% and the absence of H₂O₂ as the 100%. The IC₅₀ was calculated by establishing a sigmoid curve of the % of MPO inhibition as a function of compound concentration. The significance of the mean inhibitory curve for the inhibition in the MPO-chlorinating activity assay was tested by fitting the curve with a three-parameter sigmoid model. Results were considered as statistically significant at $P < 0.05$. In this assay, a myeloperoxidase batch with the following characteristics was used: 0.42 mg/mL, 60 U/mg, 25.2 U/mL. The scavenging activity toward HOCl was simultaneously monitored at relevant pharmacological concentrations. The reaction mixture contained the following reagents, at the concentrations stated between brackets, in a final volume of 1.0 mL: pH 7.4 phosphate buffer (PO₄³⁻ 10 mM/NaCl 300 mM), taurine (15 mM), and flufenamic acid analogs (0.5, 1, 2, 4 µM). When necessary, the volume was adjusted to 1.0 mL with water. The mixture was incubated at 37 °C and the reaction was initiated by the addition of HOCl (60 µM). After 5 min, 100 µl of catalase (4 U/µl) was added. Finally, the quantity of taurine chloramine was measured by the addition of 750 µl of 0.45 mM TNB and 2150 µl of water. The percentages of HOCl scavenged were calculated by taking the absence of inhibitor as the 0% and the absence of HOCl as the 100%. The results were expressed as means ± SD of the percentage of HOCl scavenged for at least five different determinations for each examined drug.

4.11.4. Accumulation of compound II in the presence or the absence of chloride. The interaction of the drugs with the native enzyme and its different oxidized forms was assessed by measuring compound II lifetime in two dif-

ferent conditions consisting in the presence or the absence of Cl⁻. The method was adapted from Nève et al.¹¹ In a 1.5 mL quartz cell, the following reagents were introduced, at a final concentration stated between brackets, in a final volume of 1.0 mL: 100 µl of MPO (~767 nM), 400 µl of pH 7.4 KH₂PO₄/KOH phosphate buffer (10 mM) with or without NaCl (300 mM or 0 mM), 250 µl of a drug solution (500 µM), and 50 µl of water. The reaction was initiated by addition of 100 µl of H₂O₂ (30 µM) and absorbances were simultaneously monitored with a diode-array spectrophotometer (Agilent 8453, Palo Alto, CA, USA) at wavelength characteristic for compound II (456/575 nm) and of the native enzyme (430/625 nm). Compound II lifetime was measured as the time for intersection of absorbance curves at 430 nm and 456 nm or 575 nm and 625 nm in the presence of a drug inducing an inhibition of MPO-chlorinating activity. This time corresponds to the complete conversion of compound II to native enzyme, which is demonstrated by a shift in the enzyme spectrum. The results are the means of three-independent values and are expressed as a relative value compared to the compound II lifetime in the presence of flufenamic acid. In this assay, a MPO batch with the following characteristics was used: 0.644 mg/mL, 70.8 U/mg, 46 U/mL.

4.11.5. Inhibition of LDL oxidation. The LDL oxidation was carried out at 37 °C in a final volume of 500 µl. The reaction mixture contained the following reagents at the final concentrations indicated between brackets: pH 7.2 PBS buffer, MPO (1 µg/mL), LDL (1000 µg/mL), 2 µl of HCl 1 N (4 mM), one of the drugs at different concentrations (5, 15, 30, 300 µM), and H₂O₂ (100 µM). The reaction was stopped after 5 min by cooling the tubes in ice.

In order to specifically measure the LDL oxidation due to the MPO/H₂O₂/Cl⁻ system, a recently developed ELISA was used, based on the binding between a mouse monoclonal antibody (Mab AG9) specifically recognizing the oxidized APO B-100 on LDL and an anti-mouse immunoglobulin G (Ig G) coupled with alkaline phosphatase.⁷ However, until now, the chemical structure of the epitope recognized by our antibodies has not been elucidated. The amount of oxidized LDL is quantified by measurement of the phosphatase activity and expressed as the absorbance value of the reaction product of the alkaline phosphatase, that is, *para*-nitrophenol (405 nm).

The assay was performed as described by Moguilevsky et al.⁶ in a NUNC maxisorp plate (VWR, Zaventem, Belgium): 200 ng/well of LDL was coated overnight at 4 °C in a sodium bicarbonate pH 9.8 buffer (100 µl). Afterward, the plate was washed with TBS 80 buffer and then saturated during 1 h at 37 °C with the PBS buffer containing 1% of BSA (150 µl/well). After washing the wells twice with the TBS 80 buffer, the monoclonal antibody Mab AG9 (200 ng/well), obtained according to a standard protocol and as previously described,⁶ was added as a diluted solution in PBS buffer with 0.5% of BSA and 0.1% of Polysorbate 20. After incuba-

tion during 1 h at 37 °C, the plate was washed four times with the TBS 80 buffer and a 3000 times diluted solution of Ig G anti-mouse Alkaline Phosphatase (Promega, Leiden, The Netherlands) in the same buffer was added (100 µl/well). The wells were washed again four times and a revelation solution (150 µl/well) containing 5 mg of paranitrophenyl phosphate in 5 mL of diethanolamine buffer was added for 30 min at room temperature. The reaction was stopped with 60 µl/well of NaOH 3 N solution. The measurement of the absorbance was performed at 405 nm with a background correction at 655 nm with a Bio-Rad photometer for a 96-well plate (Bio-Rad laboratories, CA, USA). Results were expressed as means ± SD of the percentage of LDL oxidation for six-independent measurements.⁶

Acknowledgment

Martine Prévost is Maître de recherche au FNRS (Belgian Research National Fund).

References and notes

- Klebanoff, S. J. *J. Leukoc. Biol.* **2005**, *77*, 598.
- Nurcombe, H. L.; Bucknall, R. C.; Edwards, S. W. *Ann. Rheum. Dis.* **1991**, *50*, 237.
- Malle, E.; Waeg, G.; Schreiber, R.; Gröne, E. F.; Sattler, W.; Gröne, H.-J. *Eur. J. Biochem.* **2000**, *267*, 4495.
- Choi, D.-K.; Pennathur, S.; Perier, C.; Tieu, K.; Teismann, P.; Wu, D.-C.; Jackson-Levis, V.; Vila, M.; Vonsattel, J. P.; Heinecke, J. W. *J. Neurosci.* **2005**, *25*, 6594.
- Carr, A. C.; Decker, E. A.; Park, Y.; Frei, B. *Free Radic. Biol. Med.* **2001**, *31*, 62.
- Moguilevsky, N.; Zouaoui Boudjeltia, K.; Babar, S.; Delrée, P.; Legssyer, I.; Carpentier, Y.; Vanhaeverbeek, M.; Ducobu, J. *Biochem. Biophys. Res. Commun.* **2004**, *323*, 1223.
- Zouaoui Boudjeltia, K.; Legssyer, I.; Van Antwerpen, P.; Kisoka, R. L.; Babar, S.; Moguilevsky, N.; Delree, P.; Ducobu, J.; Remacle, C.; Vanhaeverbeek, M.; Brohee, D. *Biochem. Cell Biol.* **2006**, *84*, 805.
- Zheng, L.; Settle, M.; Brubaker, G.; Schmitt, D.; Hazen, S. L.; Smith, J. D.; Kinter, M. *J. Biol. Chem.* **2005**, *280*, 38.
- Soyer, Z.; Bas, M.; Pabuccuoglu, A.; Pabuccuoglu, V. *Arch. Pharm.* **2005**, *338*, 405.
- Kettle, A.; Tiden, A.-K. PCT Int. Pat. 2005037835; 2005.
- Nève, J.; Parij, N.; Moguilevsky, N. *Eur. J. Pharmacol.* **2001**, *417*, 37.
- Van Antwerpen, P.; Dufasne, F.; Lequeux, M.; Zouaoui Boudjeltia, K.; Legssyer, I.; Babar, S.; Moreau, P.; Moguilevsky, N.; Vanhaeverbeek, M.; Ducobu, J.; Neve, J. *Eur. J. Pharmacol.* **2007**, *570*, 235.
- Blair-Johnson, M.; Fiedler, T.; Fenna, R. *Biochemistry* **2001**, *40*, 13990.
- Davey, C. A.; Fenna, R. E. *Biochemistry* **1996**, *35*, 10967.
- Hardy, L. W.; Malikayil, A. *Curr. Drug Discov.* **2003**, *3*, 15.
- Van Antwerpen, P.; Zouaoui Boudjeltia, K.; Babar, S.; Legssyer, I.; Moreau, P.; Moguilevsky, N.; Vanhaeverbeek, M.; Ducobu, J.; Nève, J. *Biochem. Biophys. Res. Commun.* **2005**, *337*, 82.
- Friesner, R. A.; Banks, J. L.; Murphy, R. B.; Halgren, T. A.; Klicic, J. J.; Mainz, D. T.; Repasky, M. P.; Knoll, E. H.; Shelley, M.; Perry, J. K.; Shaw, D. E.; Francis, P.; Shekin, P. S. *J. Med. Chem.* **2004**, *47*, 1739.
- Poulos, T. L.; Kraut, J. *J. Biol. Chem.* **1980**, *255*, 8199.
- Sadighi, J. P.; Harris, M. C.; Buchwald, S. L. *Tetrahedron Lett.* **1998**, *39*, 5327.
- Hosangadi, B. D.; Dave, R. H. *Tetrahedron Lett.* **1996**, *37*, 6375.
- Su, Q.; Panek, J. S. *J. Am. Chem. Soc.* **2004**, *126*, 2425.
- Chang, J.; Guo, X.; Cheng, S.; Guo, R.; Chen, R.; Zhao, K. *Bioorg. Med. Chem. Lett.* **2004**, *14*, 2131.
- Hartwell, J. L. In *Organic Syntheses*; Wiley: New York, 1944; Vol. 24, pp 22–24.
- Perez-Alvarez, M.; Raymo, F. M.; Rowan, S. J.; Shiraldi, D.; Fraser Stoddart, J.; Wang, Z.-H.; White, A. J. P.; Williams, D. J. *Tetrahedron* **2001**, *57*, 3799.
- Nishimura, S. In *Handbook of Heterogeneous Catalytic Hydrogenation for Organic Synthesis*; Wiley: New York, 2001; p 584.
- Carrico, D.; Ohkanda, J.; Kendrick, H.; Yokoyama, K.; Blaskovitch, M. A.; Bucher, C. J.; Croftner, F. S.; Van Voorhis, W. C.; Chakrabarti, D.; Buck, S. L.; Gelb, M. H.; Sebt, S. M.; Hamilton, A. D. *Bioorg. Med. Chem.* **2004**, *12*, 6517.
- Marquez, L. A.; Huang, J. T.; Dunford, H. B. *Biochemistry* **1994**, *33*, 1447.
- Arnhold, J.; Furtmüller, P. G.; Obinger, C. *Redox Rep.* **2003**, *8*, 179.
- Furtmüller, P. G.; Burner, U.; Jantschko, W.; Regelsberger, G.; Obinger, C. *FEBS Lett.* **2000**, *484*, 139.
- Kettle, A. J.; Winterbourn, C. C. *Biochem. J.* **1988**, *252*, 529.
- Burner, U.; Jantschko, W.; Obinger, C. *FEBS Lett.* **1999**, *443*, 290.
- Furtmüller, P. G.; Obinger, C.; Huanyu, Y.; Dunford, H. B. *Eur. J. Biochem.* **2000**, *267*, 5858.
- Sadowski, J.; Gasteiger, J. *Chem. Rev.* **1993**, *93*, 2567.
- Eldridge, M. D.; Murray, C. W.; Auton, T. R.; Paolini, G. V.; Mee, R. P. *J. Comput. Aided Mol. Des.* **1997**, *11*, 425.
- von Boltze, K.-H.; Bäcker, U.; Kreisfeld, H. *Arzneim.-Forsch.* **1982**, *32*, 183.
- Williams, F. J.; Relles, H. M.; Manello, D. P. E. *J. Org. Chem.* **1977**, *42*, 3419.
- Burkartmaier, A.; Mutschler, E. *Arch. Pharm.* **1978**, *311*, 161.
- Superimposed with solvent signal.
- Signal for C5' overlapped by another one between 126 and 130 ppm.
- Since this reaction was strongly exothermic, it is recommended to carefully follow the described procedure.
- J_{C-F} impossible to determine because of superimposed signals.
- Beers, R. J.; Sizer, I. W. *J. Biol. Chem.* **1952**, *195*, 133.
- Gressier, B.; Lebegue, N.; Brunet, C.; Luyckx, M.; Dine, T.; Cazin, M.; Cazin, J. C. *Pharm. World Sci.* **1995**, *3*, 76.
- Ching, T. L.; De Jong, J.; Bast, A. *Anal. Biochem.* **1994**, *218*, 377.
- Moguilevsky, N.; Garcia-Quintana, L.; Jacquet, A.; Tournay, C.; Fabry, L.; Pierard, L.; Bollen, A. *Eur. J. Biochem.* **1991**, *197*, 605.
- Hewson, W. D.; Hager, L. P. *J. Biol. Chem.* **1979**, *254*, 3175.
- Havel, R. J.; Eder, H. A.; Bragdom, J. H. *J. Clin. Invest.* **1955**, *34*, 1345.
- Peterson, G. L. *Anal. Biochem.* **1977**, *83*, 346.